First Cdc7 Kinase Inhibitors: Pyrrolopyridinones as Potent and Orally Active Antitumor Agents. 2. Lead Discovery†

Maria Menichincheri,‡ Alberto Bargiotti,‡ Jens Berthelsen,‡ Jay A. Bertrand,‡ Roberto Bossi,‡ Antonella Ciavolella,‡ Alessandra Cirla,‡ Cinzia Cristiani,‡ Valter Croci,‡ Roberto D'Alessio,‡ Marina Fasolini,‡ Francesco Fiorentini,‡ Barbara Forte,‡ Antonella Isacchi,‡ Katia Martina,§ Antonio Molinari,§ Alessia Montagnoli,‡ Paolo Orsini,‡ Fabrizio Orzi,‡ Enrico Pesenti,‡ Daniele Pezzetta,‡ Antonio Pillan,‡ Italo Poggesi,|| Fulvia Roletto,‡ Alessandra Scolaro,‡ Marco Tatò,‡ Marcellino Tibolla,‡ Barbara Valsasina,‡ Mario Varasi,⊥ Daniele Volpi,‡ Corrado Santocanale,‡,# and Ermes Vanotti*,‡

Nerviano Medical Sciences Srl, Viale Pasteur 10, 20014 Nerviano, Milano, Italy, Dipartimento di Chimica IFM, Università di Torino, Torino, Italy, GlaxoSmithKline S.p.A., Verona, Italy, Genextra Group S.p.A., Milano, Italy, National Centre for Biomedical Engineering and Sciences, National University of Ireland, Galway, Ireland

Received August 1, 2008

Cdc7 kinase is a key regulator of the S-phase of the cell cycle, known to promote the activation of DNA replication origins in eukaryotic organisms. Cdc7 inhibition can cause tumor-cell death in a p53-independent manner, supporting the rationale for developing Cdc7 inhibitors for the treatment of cancer. In this paper, we conclude the structure−activity relationships study of the 2-heteroaryl-pyrrolopyridinone class of compounds that display potent inhibitory activity against Cdc7 kinase. Furthermore, we also describe the discovery of **89S**, [(*S*)-2-(2-aminopyrimidin-4-yl)-7-(2-fluoro-ethyl)-1,5,6,7-tetrahydropyrrolo[3,2-*c*]pyridin-4-one], as a potent ATP mimetic inhibitor of Cdc7. Compound **89S** has a K_i value of 0.5 nM, inhibits cell proliferation of different tumor cell lines with an IC_{50} in the submicromolar range, and exhibits in vivo tumor growth inhibition of 68% in the A2780 xenograft model.

Introduction

The initiation of DNA replication in eukaryotic cells requires the assembly of multiple proteins at origins together with the action of protein kinases. Among the proteins known to assemble at origins before the initiation of DNA synthesis are the origin recognition complex, Cdc6,[a] and the minichromosome maintenance complex, MCM. Together they constitute the "pre-replicative" complex that is phosphorylated in the S-phase by at least two kinases, a cyclin-dependent kinase and the Cdc7 kinase. Phosphorylation is believed to activate the MCM helicase, thus leading to the unwinding of the double-stranded DNA at origins of replication, and to the loading of DNA polymerases and accessory factors that participate in the synthesis of new DNA strands during chain elongation.[1−3]

The human Cdc7 gene was identified in the late 1990s,[4−6] and its involvement in DNA replication and cell proliferation has been demonstrated.[7−10] When it is bound to one of two regulatory subunits, Dbf4 or Drf1/Dbf4B,[7,9,11] Cdc7 is activated and is able to phosphorylate several MCM subunits with some preference for MCM2.[12] Two specific phosphorylation sites in MCM2, Ser40 and Ser53, have been linked to Cdc7 activity, and RNA interference studies have demonstrated that in vivo phosphorylation of these sites is completely dependent on Cdc7.[13,14]

We and others have previously shown that siRNA mediated Cdc7 depletion causes a differential response in normal versus tumor-cell lines: tumor cells enter apoptosis in a p53-independent manner[15] while cell cycle progression is arrested in normal cells without loss of viability.[10] At the molecular level, we found that blocking initiation of replication, in contrast to blocking DNA elongation, not only causes a failure in DNA replication but also fails to activate the critical DNA damage checkpoint, leaving open the possibility for the cell to undergo further damage and eventual death. Multiple anticancer agents that target DNA replication elongation are widely used in the clinic, among them gemcitabine, active metabolites of 5-fluorouracil, and hydroxyurea.[16] The striking differences between the cellular responses to the inhibition of Cdc7 and the inhibition of DNA replication elongation by conventional chemotherapeutics, to which tumor cells can also become resistant in multiple ways,[17,18] prompted us to search for small-molecule inhibitors of the Cdc7 kinase and to explore their potential in preclinical models as a novel class of anticancer drugs that tackle the same process through a different mechanism of action.

In a previous communication,[19] we described the discovery of 2-heteroaryl-pyrrolopyridinones as Cdc7 inhibitors, their

† PDB ID of the complex **89S**-GSK3β is 3DU8.

* To whom correspondence should be addressed. Phone +39-0331581521. Fax: +39-0331581347. E-mail: ermes.vanotti@nervianoms.com.

‡ Nerviano Medical Sciences Srl.

§ Dipartimento di Chimica IFM, Università di Torino.

|| GlaxoSmithKline S.p.A.

National Centre for Biomedical Engineering and Sciences, National University of Ireland.

⊥ Genextra Group S.p.A.

[a] Abbreviations: Cdc, cell division cycle; MK2 or MAPKAPK-2, mitogen activated protein kinase-activated protein kinase-2; Cdk, cyclin-dependent kinase; GSK, glycogen synthase kinase; TAO (or SULU) thousand and one amino acid protein; CK, casein kinase; PLK, polo-like kinase; ERK, extracellular signal-regulated kinase; PKC, protein kinase C; ABL, Abelson protein-tyrosine kinase; AKT, signal transducer and activator of transcription or protein kinase B; ALK, anaplastic lymphoma kinase; AUR, aurora; CHK, Csk homologous kinase; FGFR, fibroblast growth factor receptor; IGFR, insulin-like growth factor receptor; IKKi, IKKepsilon or I-Kappa-B kinase epsilon; IR, insulin receptor; KIT, cluster of differentiation CD117; LCK, lymphocyte-specific protein tyrosine kinase; MET, high affinity tyrosine kinase receptor for hepatocyte growth factor (HGF); NEK, NIMA-related kinase (NIMA = never in mitosis gene A); NIM, nim1/cdr1 protein; PAK, p21-activated kinase; PDGFR, platelet-derived growth factor receptor; PDK, phosphoinositide-dependent kinase; PKA, cAMP-dependent kinase; P38, cytokine suppressive anti-inflammatory drug binding protein (CSBP) and RK; RET, receptor tyrosine kinase; STLK, serine-threonine like kinase or MST, mammalian STE20-like protein; TRKA, catalytic receptor for the neurotrophin, nerve growth factor (NGF); VEGFR, vascular endothelial growth factor receptor; CDI, 1,1′-carbonyldiimidazole; EDC, *N*-(3-dimethylaminopropyl)-*N*′-ethylcarbodiimide; HOBT, 1-hydroxy benzotriazole; PAMPA, parallel artificial membrane permeation assay.

10.1021/jm800977q CCC: $40.75
Published on Web 12/30/2008

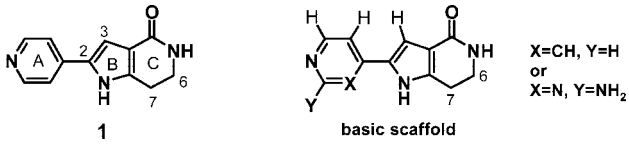

Figure 1. Pyrrolopyridinone **1** and basic scaffold.

Scheme 1. Synthesis of Pyrrolopyridinones (Method 1)[a]

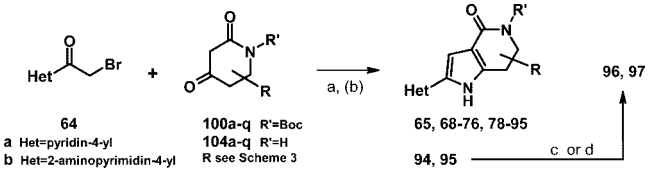

[a] Conditions: (a) NH_4OAc, EtOH, rt; (b) TFA, CH_2Cl_2, rt or 4N HCl in dioxane, MeOH, rt; (c) cyclohexene, 10% Pd−C, EtOH, reflux; (d) 1 M BCl_3 in CH_2Cl_2, −78 °C.

Scheme 2. Synthesis of Pyrrolopyridinones (method 2)[a]

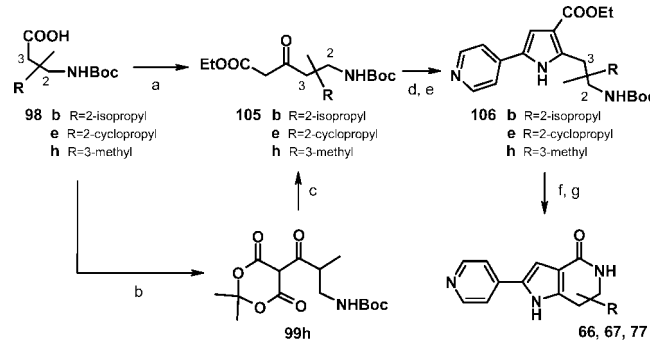

[a] Conditions: (a) $KO_2CCH_2CO_2Et$, CDI, $MgCl_2$, THF, 50 °C; (b) Meldrum's acid, DMAP, EDC·HCl, CH_2Cl_2, 0 °C; (c) EtOH, reflux; (d) 60% NaH, THF, rt, 1 h, then 0 °C, 2-bromo-1-pyridin-4-ylethanone (**64a**), THF, then rt; (e) NH_4OAc, EtOH, rt; (f) 4N HCl in dioxane, rt; (g) K_2CO_3, EtOH, reflux.

synthesis, and some details of the structure−activity relationships (SAR). We started from compound **1** (Figure 1), a scaffold formerly used for the preparation of MK2 inhibitors,[20] and by examining variations at rings A, B, and C, we outlined the basic scaffold (Figure 1) and we identified the structural features that provide the best equilibrium between activity and selectivity. In addition, we showed that compound **1** itself is able to induce cell death in a broad panel of cell lines, including cell lines resistant to other replication inhibitors, and to cause tumor growth inhibition or tumor stabilization in different preclinical tumor models.[21]

The present paper completes the SAR analysis of these molecules through the expansion of the unexplored 6 and 7 positions. Thus, a series of compounds were prepared and evaluated for their potency against a panel of 38 kinases in proliferation assays and in a variety of cell-based mechanistic assays. Next, a small subset was selected for characterization of their in vitro and in vivo pharmacological properties. Among the inhibitors synthesized, **89S** (Figure 2) stands out as having the best balance in terms of tumor target kinase inhibition profile and pharmaceutical properties for development.

Chemistry

Our strategy for the preparation of pyrrolopyridinones is based on the following two protocols (for preparation and analytical data of compounds **1** and **5** see ref 19).

1. The Hantzsch reaction was used to prepare compounds **65**, **68**−**76**, and **78**−**95** (Scheme 1).

According to this procedure, the commercially available heteroarylbromoketones **64** were reacted with piperidinediones **100** or **104** in ethanol at room temperature in the presence of ammonium acetate to obtain the final compounds **65**, **68**−**76**, and **78**−**95**. Two compounds (**96**, **97**) were obtained from **94** and **95**, respectively. *O*-Debenzylation of the side chain by hydrogenolysis of **94** afforded **96** and treatment of **95** with boron trichloride at low temperature provided **97**.

2. The intramolecular lactam ring closure of the structurally suited pyrrole precursor **106** in the very last step provided compounds **66**, **67**, and **77** (Scheme 2).

Ketoesters **105** were accessed from β-aminoacids **98** by a two-carbon extension process that was accomplished in two ways: directly, by means of monoethylmalonate potassium salt and carbonyldiimidazole in the presence of magnesium chloride,[22] or via activation with Meldrum's acid,[23] in the presence of EDC as the activating agent, followed by decarboxylation in boiling ethanol.

The preparation of the commercially unavailable precursors **106** was achieved by condensing the N-protected β-ketoesters **105** with the bromoketone **64a** and cyclizing the 1,4-diketone intermediate to the pyrrole ring under the Hantzsch reaction conditions, with ammonium acetate in ethanol at room temperature. Aminoesters **106** were finally deprotected in acid and cyclized under basic conditions, in the presence of potassium carbonate, affording pyrrolopyridinones **66**, **67**, and **77**.

For the synthesis of piperidinediones **104**, one of the three methods depicted in Scheme 3 was used.

In the first procedure, Meldrum's acid was reacted with the commercially available aminoacid derivatives **98** to obtain compounds **99**. Next, they were cyclized in boiling ethyl acetate to the protected piperidinediones **100a**−**e** that can be optionally deprotected to **104a**−**e** in acidic conditions; for instance, trifluoroacetic acid in dichloromethane. In the second procedure, β-amino-carboxyester derivatives **101** were reacted with ethyl 3-chloro-3-oxopropanoate under basic conditions, affording amides **102** that were cyclized to piperidinediones **103f**−**l** by heating in base; for example, in sodium methylate or ethylate in toluene. Their decarboxylation to piperidinediones **104f**−**l** was accomplished by refluxing in acetonitrile/water. The third alternative allows for the rapid preparation of 5-substituted analogues because each variation is obtained by simply attaching the desired chain at the preformed piperidinedione ring.[24] Commercially available *N*-Boc-piperidinedione **56** was reacted with lithium bis(trimethylsilyl)amide in tetrahydrofuran and treated with a suitable alkylating agent R-X, where X is iodo or bromo. The desired protected piperidinediones **100m**−**q** were thus provided that could be optionally deprotected to **104m**−**q** under acidic conditions such as trifluoroacetic acid in dichloromethane. The preparation of commercially unavailable β-aminoesters **101** is shown in Scheme 4.

The aminoesters were obtained as follows: **101f** by amination of ethyl 3-methyl-but-2-enoate with ammonia under pressure and heating,[25] **101j** from ethyl 2-cyano-2-ethyl-butanoate by hydrogenation catalyzed by platinum oxide, and **101g**[25] and **101l** by exhaustive catalytic hydrogenation of ethyl 2-cyano-3-methyl-2-butenoate and ethyl cyano-cyclobutylidene-acetate, respectively. Ethyl cyano-cyclobutylidene-acetate was in turn prepared from cyclobutanone and ethyl cyanoacetate under acidic conditions, with acetic acid and ammonium acetate.[26]

Results and Discussion

Having defined the basic scaffold of pyrrolopyridinones in a previous study,[19] we concentrated our effort on positions 6 and

Scheme 3. Synthesis of Piperidinediones[a]

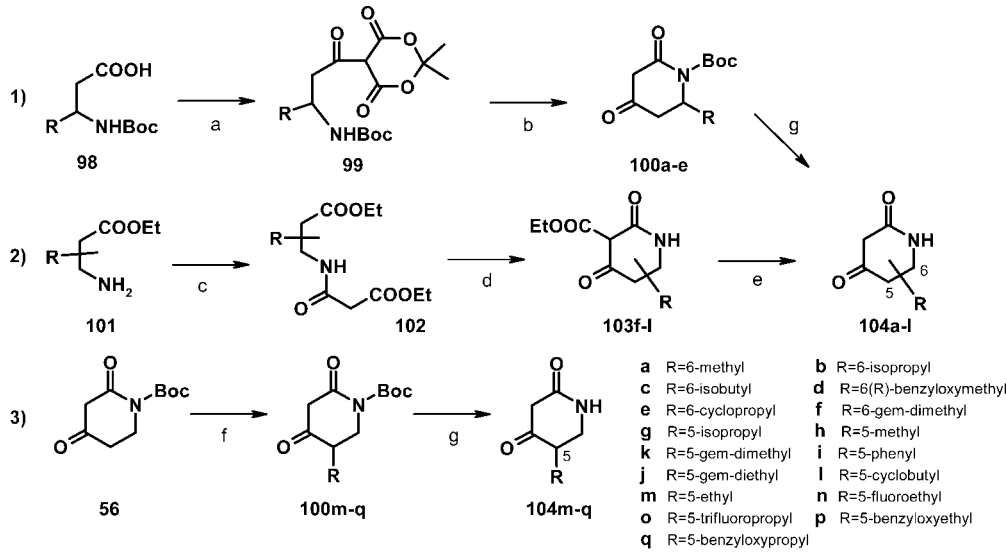

[a] Conditions: (a) Meldrum's acid, CH_2Cl_2, EDC·HCl, 0 °C then rt; (b) EtOAc, reflux; (c) $ClCOCH_2COOEt$, TEA, CH_2Cl_2, rt; (d) 25% NaOEt in EtOH, toluene, 80 °C; (e) CH_3CN, water, reflux; (f) lithium bis(trimethylsilyl)amide, THF, RX (X = I, Br), −20 °C; (g) TFA, CH_2Cl_2, rt.

Scheme 4. Synthesis of Aminoacid Derivatives[a]

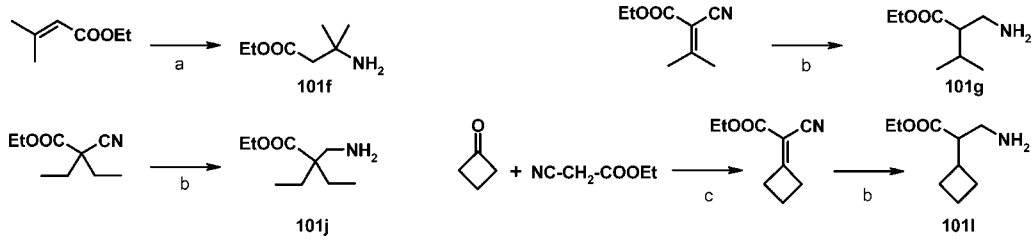

[a] Conditions: (a) EtOH, NH_3 (gas), 90 °C (sealed tube); (b) PtO_2, H_2, EtOH, 4N HCl in dioxane, rt; (c) AcOH, NH_4OAc,toluene, rt.

7. With the exclusion of gem-disubstituted analogues, the formation of new carbon−carbon bonds induced asymmetry into the molecule. The stereogenic center was created in a nonstereospecific manner and, therefore, the SAR was carried out with the racemates. Once a few molecules were chosen from the eligible candidates, chiral chromatographic separation provided the single enantiomers.

To understand the influence of substitutions at position 6, the same set of substituents was introduced and compared in the two series of pyridinyl and aminopyrimidinyl derivatives (Table 1). The substituents are almost exclusively alkyl groups, a choice dictated by the need to increase lipophilicity (cLogP is as low as −1 in the unsubstituted precursors) with the hope of improving the suboptimal cell permeability (1.84×10^{-6} cm/s measured for **1** in the PAMPA assay)[27,28] and the correlated cellular activity. Surprisingly, although different substituents gave a variation in the IC_{50} values for both series, they did not have a major influence on the cellular activity.

As for position 6, the influence of substitutions at position 7 on activity was established by introducing the same set of substituents in the two series and comparing them with the unsubstituted analogues (Table 2). In both series, the presence of the R_7 groups enhanced cellular activity: by 2−6 fold in pyridinyl analogues and by 3−8 fold in aminopyrimidinyl analogues. Comparing the same substituents (namely methyl, isopropyl and gem-dimethyl) at positions 6 and 7 of the pyridinyl (Table 3) and aminopyrimidinyl (Table 4) derivatives, it is apparent that only the substituents at position 7 ensure 2−6 fold higher cellular activity in both series.

While developing the first generation of Cdc7 inhibitors, we decided that the concomitant inhibition of other kinases involved in cell cycle regulation, such as Cdk2 and PLK1, was to be avoided as much as possible because it could potentially mask the biological effects of Cdc7 inhibition. Thus, the compounds were tested against a panel of 38 kinases to evaluate their levels of selectivity. Interestingly selectivity determinations distinguish between 7-substituted aminopyrimidinyl and pyridinyl derivatives, as the former series shows selectivity ratios greater than 30 versus Cdk2A, a kinase that frequently cross-reacts with Cdc7 inhibitors,[19] while the latter derivatives are 2−3 times less selective against Cdk2A. In the case of aminopyrimidinyls, 1 out of 38 kinases (TAO3) was inhibited at $IC_{50} < 50$ nM versus 3 out of 38 kinases (Cdk2A, GSK3β, PLK1) inhibited at $IC_{50} < 50$ nM for pyridinyls.

With the exception of the gem-dialkyl derivatives (**90**, **91**) that experience a strong loss of selectivity versus many kinases, all 7-substituted aminopyrimidinyl derivatives demonstrate an improved cell-activity/selectivity profile with respect to the unsubstituted parent compound **5**. For this reason, they were chosen for further development.

A few new derivatives carrying heteroatoms in their chains were also prepared in order to explore the sugar pocket region for additional binding interactions. As expected from the docking of compound **1** into the predicted ATP pocket of the kinase obtained from a homology model,[19] a hydroxyl group inserted in the aliphatic chain protruding from position 7 could mimic the hydroxyl groups of the ATP sugar ring and a fluoro atom could establish electrostatic interactions with the carbons of the

Table 1. SAR: Variations of Group R_6 (IC_{50}, μM)[a]

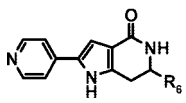
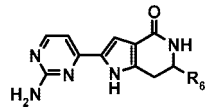

Cpd #	Cdc7	A2780[b]	R_6	Cpd #	Cdc7	A2780
1	0.010± 0.004	1.1	H	**5**	0.007± 0.001	1.7
65	0.013± 0.007	2.4		**71**	0.026± 0.003	3.9
66	0.006± 0.002	0.9		**72**	0.012± 0.007	1.3
67	0.005± 0.003	1.3		**73**	0.011± 0.008	1.1
68	0.003± 0.001	0.8		**74**	0.008± 0.005	1.6
69	0.032± 0.020	1.2		**75**	0.064± 0.051	1.8
70	0.044± 0.003	4.8		**76**	0.052± 0.028	3.0

[a] IC_{50} values are reported as the mean ± standard deviation ($n \geq 2$). [b] IC_{50} values are reported as the mean of 2−3 experiments with a coefficient of variation below 35%.

backbone carbonyls. From this limited survey, only compounds **93** and **94** emerged as acceptably active on cells (Table 5). However, although both compounds are active on cells, they demonstrate slight differences in selectivity; **93** was sufficiently selective with none out of 38 kinases inhibited at $IC_{50} < 100$ nM, while **94** inhibits 2 out of 38 kinases (Cdk2A, GSK3β) at $IC_{50} < 50$ nM.

To assess the influence of the configuration at position 7, derivatives **86**−**89** and **93** were selected for further investigations because they show acceptable cell activity with greater than 30-fold selectivity versus the other tested kinases. Thus, the racemic mixtures were separated by chiral column chromatography (see the Experimental Section) and the results were determined for the single enantiomers. As shown in Table 6, the impact of configuration on the Cdc7 activity is evident only for the isopropyl (**87**) and cyclobutyl (**88**) enantiomers. Among the most active compounds in cells **86**−**2**, **87**−**2** and **88**−**2** display poorer levels of selectivity, showing inhibition against 3 out of 38 kinases (GSK3β, PLK1, and TAO3) at $IC_{50} < 100$ nM.

Because **1** was shown to inhibit Cdk9,[21] a kinase involved in the phosphorylation of RNA polymerase II and in transcriptional regulation of gene expression,[29,30] all of the selected compounds were also tested for their capability to block Cdk9 activity in a biochemical assay. As can be seen from Table 6, most compounds inhibit Cdk9T,[31] with IC_{50} values lower than 100 nM and less than 20 times the ratio with respect to Cdc7. Thus they can be defined as dual Cdc7/Cdk9 inhibitors. No attempts have been made to define the structure−activity relationship controlling the specificity for Cdc7 over Cdk9. As

Table 2. SAR: Variations of Group R_7 (IC_{50}, μM)[a]

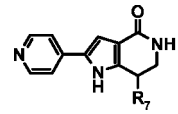
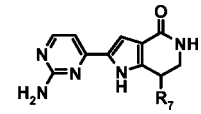

Cpd #	Cdc7	A2780[b]	R_7	Cpd #	Cdc7	A2780
1	0.010± 0.004	1.1	H	**5**	0.007± 0.001	1.7
77	0.010± 0.008	0.6		**85**	0.006± 0.004	0.7
78	0.002± 0.001	0.3		**86**	0.005± 0.002	0.4
79	0.010± 0.007	0.5		**87**	0.004± 0.002	0.4
80	0.003± 0.002	0.5		**88**	0.005± 0.001	0.3
81	0.002± 0.001	0.6		**89**	0.003± 0.001	0.6
82	0.003± 0.002	0.2		**90**	0.002± 0.001	0.3
83	0.006± 0.001	0.2		**91**	0.005± 0.003	0.2
84	0.020± 0.015	4.0		**92**	0.019± 0.011	3.0

[a] IC_{50}values are reported as the mean ± standard deviation ($n \geq 2$). [b] IC_{50} values are reported as the mean of 2−3 experiments with a coefficient of variation below 35%.

mentioned in previous work,[21] Cdk9 does not appear to be strictly essential for cell cycle division and the combination of transcriptional Cdk inhibition with either cell cycle or other types of cellular stress represents an opportunity for tackling leukemia and solid tumors. For these reasons, we do not consider the inhibitory activity on Cdk9 kinase as a limitation and, consequently, the choice of the compounds for development was not influenced by these observations.

The most promising compounds from Table 6, **86**−**1**, **89S**, and **93**−**2**, were chosen for additional investigation and their in vitro physicochemical ADME properties were determined (Table 7). Interestingly, these compounds are not distinguished by their in vitro parameters because they all are acceptably soluble, poorly permeable, metabolically stable, and only moderately bound to plasma proteins. In contrast, the in vivo results are more helpful because they suggest an overall superiority of compound **89S** after intravenous (iv) and oral (po) administration (Table 8).

Compound **89S** displayed high clearance (3.7 L/h/kg), yet it was lowest among compounds tested. Compound **89S** also had the highest volume of distribution at about 4-fold total body water, indicating extensive tissue distribution. Plasma levels for **89S** were detectable up to 6 h *post*dosing, giving an apparent average terminal half-life of about 1 h, and the greatest AUC

Table 3. SAR: Influence of Position of Group R in the Pyridinyl Series (IC_{50}, μM)[a]

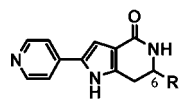
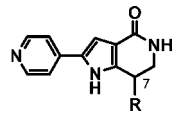

R	Cpd #	Cdc7	A2780[b]	Cpd #	Cdc7	A2780
H	**1**	0.010± 0.004	1.1	**1**	0.010± 0.004	1.1
	**65**	0.013± 0.007	2.4	**77**	0.010± 0.008	0.6
	66	0.006± 0.002	0.9	**79**	0.010± 0.007	0.5
	69	0.032± 0.020	1.2	**82**	0.003± 0.002	0.2

[a] IC_{50} values are reported as the mean ± standard deviation ($n \geq 2$). [b] IC_{50} values are reported as the mean of 2−3 experiments with a coefficient of variation below 35%.

Table 4. SAR: Influence of Position of Group R in the Aminopyrimidinyl Series (IC_{50} μM)[a]

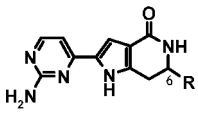
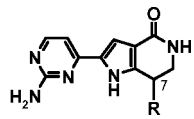

R	Cpd #	Cdc7	A2780[b]	Cpd #	Cdc7	A2780
H	**5**	0.007± 0.001	1.7	**5**	0.007± 0.001	1.7
	71	0.026± 0.003	3.9	**85**	0.006± 0.004	0.7
	72	0.012± 0.007	1.3	**87**	0.004± 0.002	0.4
	**75**	0.064± 0.051	1.8	**90**	0.002± 0.001	0.3

[a] IC_{50} values are reported as the mean ± standard deviation ($n \geq 2$). [b] IC_{50} values are reported as the mean of 2−3 experiments with a coefficient of variation below 35%.

(9.5 μM.h) after iv dosing. After po dosing, the T_{max} of compound **89S** was found to be 0.5 h, the terminal half-life was comparable to that after iv administration, suggesting that the rate of absorption does not interfere with the disposition of the compound, and the oral bioavailability was acceptable (F = 53%). Most important, **89S** showed the greatest AUC (5.0 μM·h). The pharmacokinetic properties of compound **89S** were also assessed in Han-Wistar rats and in beagle dogs following both iv and po dosing (Table 9). After iv dosing in the rat, the compound displayed moderate clearance (1.8 L/h/kg) and a volume of distribution three times the total body water. After po dosing, detectable plasma levels were observed up to 24 h post dosing and the T_{max} of the compound was found to be 0.25 h with acceptably high bioavailability (F = 45%). In dogs, the

Table 5. SAR: Variations of Group R_7 in the Aminopyrimidinyl Series (IC_{50} μM)[a]

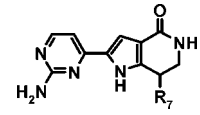

Cpd #	R_7	Cdc7	A2780[b]	Cpd #	R_7	Cdc7	A2780
5	H	0.007± 0.004	1.7	**95**		0.024± 0.010	2.0
93		0.010± 0.004	0.5	**96**		0.004± 0.002	1.1
94		0.007± 0.005	0.4	**97**		0.012± 0.007	6.0

[a] IC_{50} values are reported as the mean ± standard deviation ($n \geq 2$). [b] IC_{50} values are reported as the mean of 2−3 experiments with a coefficient of variation below 35%.

compound showed moderate-high clearance (3.2 L/h/kg) and a volume of distribution three times the total body water. Furthermore, in dogs, the renal clearance accounted for approximately 13% of the total clearance. After po dosing, the T_{max} of the compound was found to be 0.3 h and the extent of the absorption was reasonable (F = 50%).

Because of the characteristics described above, **89S** was selected for further in vitro and in vivo testing. As such, **89S** was tested against a broader panel of tumor cell lines and found to be active against many of them. The observed potency was comparable to that observed against A2780 cells and **89S** was always more potent than compound **1** (Table 10). Thus, further in vitro investigation was directed at demonstrating that the antiproliferative activity observed was mediated by Cdc7 inhibition. The compound was checked for its capacity to block the cell cycle and stop DNA synthesis by bromodeoxyuridine (BrdU) incorporation block. The cell cycle profile was studied on asyncronous HeLa cells, using fluorescence activated cell sorting (Figure 3). Cell population peaks showed a G1/S block to DNA content analysis showed accumulation of S-phase cells at 3 μM, with drastic decrease of bromodeoxyuridine incorporation (from 35% to 3%), meaning that DNA synthesis in these tumor cells was impaired. Western blot analysis of the phosphorylation status of the known substrate MCM2[12] showed a corresponding inhibition of phosphorylation at the Cdc7 dependent sites Ser40 and Ser53,[13] indicating that the antiproliferative activity of **89S** is mediated by blocking Cdc7.

Caspase 3 activation and sub-G1 accumulation indicate that the treatment with **89S** causes apoptosis in the cells (Figure 4). Figure 5 shows that the minimum dose necessary to achieve Cdc7 kinase inhibition, after 4 h of treatment of A2780 cells with **89S**, was 0.6 μM, corresponding to the IC_{50} of proliferation in this cell line. This result indicates that the mechanism of action of the compound strongly correlates with Cdc7 inhibition. These features, coupled with good solubility in vehicles (10 mg/mL in 5% dextrose, in 5% Tween 80 in dextrose solution, and in 50% PEG 400 in dextrose solution), excellent metabolic stability (CL_{int} is 0.3 L/h/kg at the concentration of 1 μM in rat hepatocytes and no inhibition of the major human cytochrome P450 isoforms CYP1A2, CYP2C8, CYP2C9, CYP2C19,

Table 6. SAR: Influence of C-7 Configuration in the Aminopyrimidinyl Series (IC_{50} μM)[a]

Cpd #	Structure	Cdc7	Cdk9T	A2780[b]	Cpd #	Structure	Cdc7	Cdk9T	A2780
1	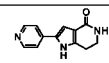	0.010± 0.004	0.034± 0.007	1.1	**88-1***	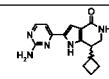	0.011± 0.006	0.083± 0.001	1.3
5	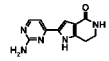	0.007± 0.001	0.029± 0.005	1.7	**88-2***		0.002± 0.002	0.096± 0.008	0.2
86-1*	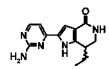	0.004± 0.003	0.073± 0.028	0.4	**89R#**	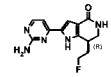	0.005± 0.004	0.096± 0.015	1.0
86-2*		0.005± 0.002	0.017± 0.001	0.4	**89S#**	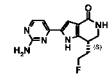	0.002± 0.001	0.028± 0.004	0.5
87-1*	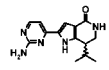	0.013± 0.003	0.031± 0.004	1.0	**93-1***	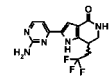	0.012± 0.004	0.218± 0.075	1.0
87-2*		0.001± 0.002	0.073± 0.026	0.6	**93-2***		0.011± 0.003	0.395± 0.101	0.3

[a] IC_{50} values are reported as the mean ± standard deviation ($n \geq 2$). * = stereochemistry not determined; # = absolute configuration assigned by X-ray analysis of the binary complex with GSK3β kinase (see Figure 6). [b] IC_{50} values are reported as the mean of 2−3 experiments with a coefficient of variation below 35%.

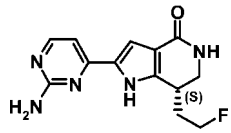

Figure 2. Structure of Pyrrolopyridinone **89S**.

CYP2D6, CYP3A4 at 100 μM is displayed) and good selectivity (Table 11), make compound **89S** suitable for efficacy trials.

The absolute configuration of the molecule was assigned by X-ray analysis of the binary complex with GSK3β and turned out to be (S) (Figure 6). The binding mode of the crystallographic structure of compound **89S** in complex with GSK3β validates the modeling hypothesis formulated with the homology model of Cdc7 reported in a previous communication,[19] where the binding of the nitrogen of pyridine with the hinge region was found to be the more favorable of the two possible modes.

In vivo, **89S** proved to be efficacious in the human ovarian A2780 xenograft mouse model and in the 7,12-dimethylbenz(*a*)anthracene (DMBA) induced rat tumor model.

In the A2780 xenograft model (Figure 7), tested orally at 60 mg/kg twice a day for 10 days, the compound showed 68% tumor growth inhibition. This dose is potentially very close to the maximal tolerated dose as the mice experienced severe, although reversible, body weight loss.

With the aim of providing a quantitative estimate of the in vivo potency, a pharmacokinetic and pharmacodynamic approach, based on a previously published model,[32] was applied to the efficacy data. This method, linking the pharmacokinetics of the compound to the effect on the growth curves, provides two model parameters: *Ct* and K_2 (Table 12). The former (*Ct*) provides an estimate of the steady-state drug concentration in plasma above which tumor mass reduction and eventually eradication are observed, the latter (K_2) can be regarded as a drug specific measurement of the potency of the compound. Both model parameters indicate a good in vivo potency of **89S**. The estimated *Ct* value in the A2780 xenograft model was 1.93 μmol/L and the potency K_2 was 0.0059 h/μmol/L. As a comparison, the same parameters for a well-known antitumor drug like Paclitaxel are 0.545 μmol/L and 0.022 h/μmol/L, respectively.[32]

In the DMBA tumor model, **89S** was tested at a dose of 20 mg/kg, oral, twice a day for 10 days. As displayed in Figure 8, durable tumor stabilization is reached.

Thus, **89S** appears to have a greater antitumor activity than compound **1**,[21] both in the A2780 ovary carcinoma xenograft (68% vs 50% tumor growth inhibition) and in the DMBA tumor model, where tumor stabilization is maintained for a longer period of time (35 vs 25 days).

To correlate antitumor activity with Cdc7 inhibition, A2780 tumors, explanted from controls or animals treated with two administrations (60 mg/kg each) of **89S** in 6 h (second administration 3 h after the first one), were analyzed by Western blot (Figure 9).

We observed that phosphorylation of Mcm2 at the Cdc7 dependent sites Ser40 and Ser53 was greatly decreased in the tumors of treated animals consistent with inhibition of Cdc7 in the tumor cells.

Conclusions

Pyrrolopyridinones have been shown to be potent inhibitors of the Cdc7 kinase. Our investigation of the SAR of this series of compounds has identified the key components necessary for kinase inhibition. Optimization efforts led to (*S*)-2-(2-aminopyrimidin-4-yl)-7-(2-fluoro-ethyl)-1,5,6,7-tetrahydropyrrolo[3,2-*c*]pyridin-4-one (**89S**), which showed a number of desirable

Table 7. In Vitro ADME Parameters for Selected 7-Substituted Aminopyrimidinyl Derivatives

			metabolic stability		
compd no.	solubility pH 7 (μM)	permeability caco-2 (Papp)	Cl_{int} (L/h/kg) rat hepatocytes (1 μM)	CYP4503A4 human hepatocytes (% drug after 1 h)	PPB[a] (%)
86−1	>225	low	0.3	99	52
89S	>225	low	0.3	95	45
93−2	195	low	0.5	94	58

[a] Plasma protein binding.

Table 8. Mean ± SD Pharmacokinetic Parameters for Selected 7-Substituted Aminopyrimidinyl Derivatives Following iv Single Dose and Oral Single Dose, in Harlan nu/nu Mice[a]

	in vivo ADME parameters (nude mice)[a]									
	PK data (iv), dose[b]: 10 mg/kg					PK data (po), dose[b]: 10 mg/kg				
compd no.	C_{max} (μM)	AUC_∞ (μM·h)	CL (L/h/kg)	V_{ss} (L/kg)	$t_{1/2}$ (h)	C_{max}	T_{max} (h)	AUC_∞	$t_{1/2}$	F^c (%)
86−1	12.6 ± 1.2	4.9 ± 0.6	7.5 ± 0.8	1.5 ± 0.1	0.2 ± 0.01	2.7 ± 0.4	0.34 ± 0.1	3.6 ± 0.2	1.3 ± 0.1	74
89S	20.3 ± 6.9	9.5 ± 3.3	3.7 ± 1.1	2.6 ± 1.3	1.0 ± 0.1	2.6 ± 0.5	0.5 ± 0.0	5.0 ± 0.1	1.0 ± 0.1	53
93−2	13.6 ± 2.1	5.3 ± 0.9	5.3 ± 0.8	1.5 ± 0.7	0.9 ± 0.6	0.8 ± 0.2	0.33 ± 0.1	1.7 ± 0.1	1.7 ± 0.1	31

[a] $n = 6$ animals per study. [b] Dosed in 5% dextrose. [c] Bioavailability.

Table 9. Mean ± SD Pharmacokinetic Parameters of **89S** Following iv Single Dose and Oral Single Dose to Han-Wistar Rats ($n = 3$ for Each Leg) and Beagle Dogs ($n = 2$ for Each Leg in a Crossover Design)

	in vivo ADME parameters										
	PK data (iv), dose[c]: 10 mg/kg						PK data (po), dose[c]: 20 mg/kg				
rat[a]	C_{max} (μM)	AUC_∞ (μM·h)	CL (L/h/kg)	CL_r	V_{ss} (L/kg)	$t_{1/2}$ (h)	C_{max}	T_{max} (h)	AUC_∞	$t_{1/2}$	F^d (%)
	15.7 ± 2.5	19.9 ± 7.2	1.8 ± 0.6	1.1 ± 0.2	2.1 ± 0.7	1.3 ± 0.6	2.0 ± 0.7	0.3 ± 0.0	18.9 ± 5.6	6.2 ± 1.7	33−45
	PK data (iv), dose[c]: 5 mg/kg						PK data (po), dose[c]: 10 mg/kg				
dog[b]	C_{max} (μM)	AUC_∞ (μM·h)	CL (L/h/kg)	CL_r	V_{ss} (L/kg)	$t_{1/2}$ (h)	C_{max}	T_{max} (h)	AUC∞	$t_{1/2}$	F^d (%)
	8.9±0.4	6.3±1.2	3.2±0.4	0.4±0.2	2.1±0.2	0.6±0.1	5.5±2.2	0.3±0.1	6.4±2.0	1.2±0.2	51

[a] $n = 6$ animals per study. [b] $n = 4$ animals per study. [c] Dosed in 5% dextrose. [d] Bioavailability.

Table 10. Antiproliferative Activity of Compound **89S** (in Square Brackets Compound **1**)

cell line	origin	IC_{50} (μM)[a]	cell line	origin	IC_{50} (μM)
A2780	ovary	0.5[1.1]	SW48	colon	0.9 [1.2]
MCF7	mammary	1.1 [1.3]	L363	AML	1.3 [1.6]
COLO205	colon	0.5 [1.5]	NCI-H929	myeloma	1.2 [1.8]
HCT116	colon	0.4 [1.0]	OPM2	myeloma	3.7 [4.5]
HT29	colon	4.1 [5.0]	NHDF	human fibroblasts	1.6 [1.6]
SW403	colon	0.6 [1.0]	NIH-3T3	mouse fibroblasts	2.5 [−]

[a] IC_{50} values are reported as the mean of 2−3 experiments with a coefficient of variation below 35%.

features for the purpose of cancer drug development, including biochemical potency against its main target, acceptable selectivity against a panel of unrelated kinases, as well as good potency in proliferation and in cell-based mechanistic assays. Compound **89S** displayed good bioavailability across multiple species, resulting in plasma exposures sufficient to achieve good antitumor activity in two different species. Altogether, these characteristics make **89S** a significantly improved derivative with respect to the starting parent compound **1**. However, **89S**, like **1** and many other compounds in this class, is rapidly cleared from plasma. Defining the mechanisms for plasma clearance and being able to limit it will be a critical challenge for developing a Cdc7 kinase inhibitor from this class that is suitable for human administration.

Experimental Section

1. Chemistry. Unless otherwise noted, all solvents and reagents were obtained from commercial suppliers and used without further purification.

All reactions involving air- or moisture-sensitive reagents were performed under an argon atmosphere. All final compounds were purified to >95% purity as determined by high-performance liquid chromatography (HPLC).

Purity was routinely measured by HPLC on a Waters X Terra RP 18 (4.6 mm × 50 mm, 3.5 μm) column using a Waters 2790 HPLC system equipped with a 996 Waters PDA detector and Micromass model A ZQ single quadrupole mass spectrometer, equipped with an electrospray (ESI) ion source. Mobile phase A was an ammonium acetate 5 mM buffer (pH 5.5 with acetic acid/acetonitrile 95:5), and mobile phase B was H_2O/acetonitrile (5:95). The following conditions were used: a gradient from 10 to 90% B in 8 min and held at 90% B for 2 min; UV detection at 220 and 254 nm; a flow rate of 1 mL/min; an injection volume of 10 μL; full scan, mass range from 100 to 800 amu. The capillary voltage was 2.5 kV; the source temperature was 120 °C; the cone was 10 V. Retention times (HPLC rt) are given in minutes at 220 or at 254 nm. Masses are given as an *m*/*z* ratio.

When necessary, compounds were purified by preparative HPLC on a Waters Symmetry C18 (19 mm × 50 mm, 5 μm) column using a Waters preparative HPLC 600 equipped with a 996 Waters PDA detector and a Micromass model A ZMD single quadrupole mass spectrometer, with electrospray ionization, in the positive mode, was used. Mobile phase A was water and 0.01% trifluoroacetic acid, and mobile phase B was acetonitrile. The following conditions were used: a gradient from 10 to 90% B in 8 min and held at 90% B for 2 min; a flow rate 20 mL/min.

Column chromatography was conducted either under medium pressure on silica (Merck silica gel 40−63 μm) or on prepacked silica gel cartridges (Biotage) or on a Horizon system.

^{1}H NMR spectra were routinely recorded on a Varian Inova 400 spectrometer operating at 400 MHz and equipped with a 5 mm indirect detection PFG probe, (^{1}H{^{15}N-^{31}P}). Where reported, a Varian Inova 500 spectrometer, operating at 500 MHz and equipped with a 5 mm triple resonance PFG probe, (^{1}H{^{15}N-^{31}P}) or a Varian Mercury 300 spectrometer, operating at 300 MHz and equipped with a 5 mm switchable probe (^{15}N-^{31}P{^{1}H,^{19}F}) was used. All observed protons are reported as parts per million (ppm) downfield from tetramethylsilane (TMS) or other internal reference in the appropriate solvent indicated. Data are reported as follows: chemical

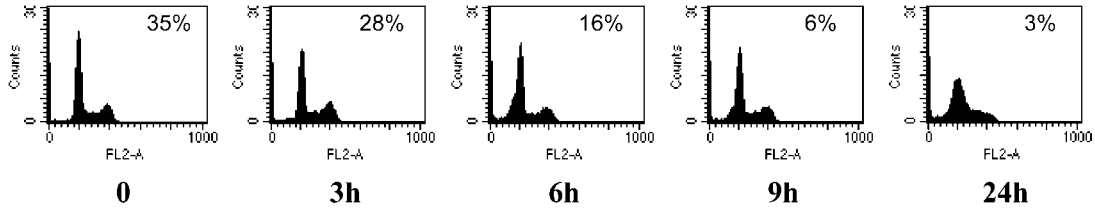

Figure 3. DNA content and BrdU incorporation analysis in HeLa cells treated with compound **89S**. Logarithmically growing HeLa cells were treated for the indicated times with 3 μM **89S** and labeled with BrdU before fixation. DNA content and BrdU positive cells (%) were measured by FACS.

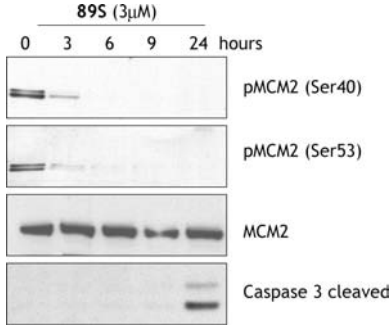

Figure 4. In vitro mechanism of action (MoA) of compound **89S**. The compound inhibits cellular Cdc7. A2780 cells were incubated for up to 24 h with 3 μM concentration of **89S**. Proteins were prepared and analyzed by Western blot. Phosphorylation status of MCM2 protein at Cdc7-dependent (Ser40, Ser53) phospho-site was assessed using specific antiphosphopeptide antibodies. Detection of cleaved caspase 3 indicates that cells are undergoing apoptotic cell death.

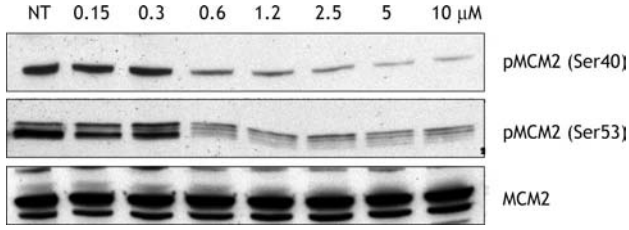

Figure 5. In vitro MoA of compound **89S**. A2780 cells were incubated for 4 h with different concentrations of **89S**. Proteins were prepared and analyzed by Western blot. Phosphorylation status of MCM2 protein at Cdc7-dependent (Ser40, Ser53) phospho-site was assessed using specific antiphosphopeptide antibodies.

Table 11. Selectivity Profile of compound **89S**[a]

kinase	IC_{50} (μM)	kinase	IC_{50} (μM)
Cdc7	0.002 ± 0.001	MK2	0.510 ± 0.135
Cdk9T	0.028 ± 0.004	PLK1	0.574 ± 0.384
Cdk1b	0.030 ± 0.004	Cdk2E	0.670 ± 0.020
TAO3	0.126 ± 0.043	ERK2	0.846 ± 0.247
Cdk2A	0.138 ± 0.055	PKCβ	1.149 ± 0.162
GSK3β	0.146 ± 0.045	Cdk5P25	1.620 ± 0.240
CK2	0.359 ± 0.120	others[b]	>4

[a] IC_{50} values are reported as the mean ± standard deviation ($n \geq 2$). [b] ABL, AKT1, ALK, AUR1, AUR2, Cdk4, CHK1, FGFR1, IGFR1, IKKi, IR, KIT, LCK, MET, NEK6, NIM1, PAK4, PDGFR, PDK1, PKAα, P38β, RET, STLK2, or MST4, TRKA, and VEGFR3.

shift, multiplicity (s = singlet, d = doublet, t = triplet, q = quartet, bs = broad singlet, bd = broad doublet, bt = broad triplet, td = triplet of doublet, ddd = doublet of doublet of doublet, *m* = multiplet), coupling constants, and number of protons.

Low-resolution mass spectral (MS) data were determined on a Finnigan MAT LCQ ion trap instrument, equipped with ESI. ESI(+) high-resolution mass spectra (HRMS) were obtained on a Waters Q-Tof Ultima directly connected with micro HPLC 1100 Agilent as previously described.[33]

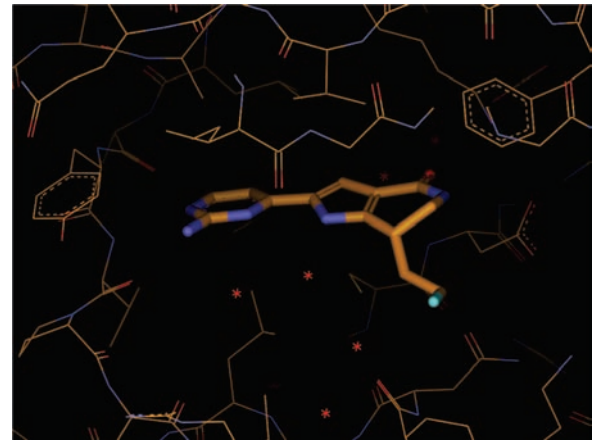

Figure 6. Close-up view of **89S** in the ATP binding pocket of GSK3β.

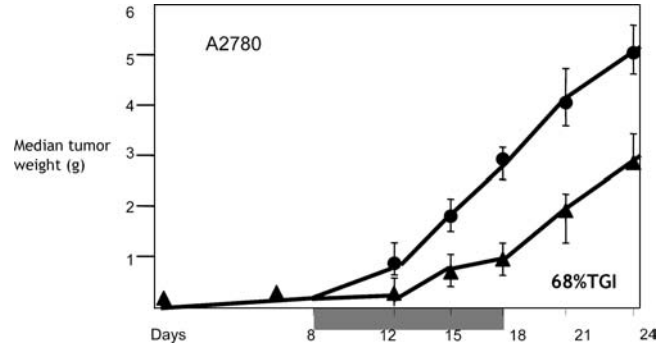

Figure 7. Compound **89S** has antitumor activity in rodents. CDI Nu/Nu mice carrying subcutaneous A2780 human ovarian carcinoma were treated with either vehicle or **89S** by oral administration. Curves indicate tumor growth in vehicle-treated (circles) or **89S**-treated mice for 10 days (gray bar) at 60 mg kg^{-1} (triangles) twice a day. Data are represented as mean ± SEM.

Table 12. Pharmacokinetic and Pharmacodynamic Parameters of **89S** after the Last Administration during a 10-Day Consecutive Treatment at the Dose of 30 mg/kg Twice a Day

parameters	value	SD	%CV
V_1 (L/kg)	166.5	26.0	15.6
K_{01} (h^{-1})	8.13	6.09	74.9
K_{10} (h^{-1})	0.09	0.01	17.1
Ct (μmol/L)	1.93		
K_2 (h/μmol/L)	0.0059		

Elemental analyses were performed on Carlo Erba EA1110 instrument, and C and N values were within ± 0.4% of theoretical values unless otherwise noted.

Thin-layer chromatography was performed on Merck silica gel 60 plates coated with 0.25 mm layer with fluorescent indicator. Components were visualized by UV light (λ = 254 and 366 nm) and iodine vapors.

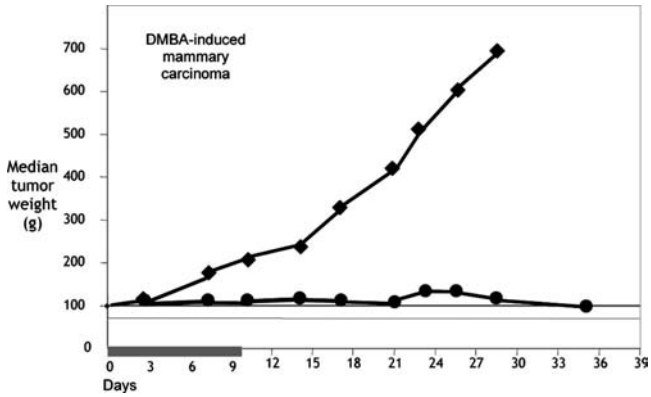

Figure 8. CD OFA rats carrying DMBA-induced mammary carcinomas were treated with either vehicle (squares) or with 20 mg kg^{-1} **89S** (circles) orally, twice a day, for 10 days (gray bar). Curves indicated median of tumor weight.

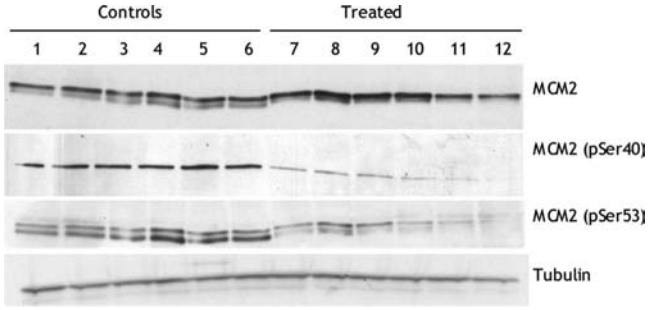

Figure 9. A2780 xenografts were treated either with vehicle (lanes 1−6) or with **89S** (lanes 7−12). Tumors were explanted and analyzed by Western blot using antibodies against phosphorylated MCM2 at Ser40 and Ser53. Levels of total MCM2 and tubulin were also measured as loading control.

Some of the racemates were resolved by HPLC separation on chiral columns. In particular, preparative columns Chiralpack AD, Chiralpack AS, and Chiralcell OJ were used.

6-Isopropyl-2-pyridin-4-yl-1,5,6,7-tetrahydropyrrolo[3,2-*c*]pyridin-4-one (66). To a suspension of 2-(2-*tert*-butoxycarbonylamino-3-methyl-butyl)-5-pyridin-4-yl-1*H*-pyrrole-3-carboxylic acid ethyl ester **106b** (6.2 g, 15.6 mmol) in dioxane (200 mL), 4 N HCl in dioxane (170 mL) was added. The solution was stirred 4 h at room temperature, then concentrated, to afford crude 1-(3-ethoxycarbonyl-5-pyridin-4-yl-1*H*-pyrrol-2-ylmethyl)-2-methyl-propyl-ammonium chloride that was dissolved into absolute ethanol (350 mL) and was heated to reflux for 72 h. The solvent was removed and to the raw product acetonitrile (10 mL), and water (200 mL) were added. The precipitate was collected, washed with water, and dried. Obtained 3.58 g (14 mmol, 90% yield) of the title compound.

^{1}H (400 MHz, DMSO-d_6) δ ppm 0.93 (d, J = 6.83 Hz, 3 H) 0.94 (d, J = 6.95 Hz, 3 H) 1.82−1.96 (m, 1 H) 2.80 (dd, J = 16.58, 9.51 Hz, 1 H) 2.91 (dd, J = 16.71, 5.73 Hz, 1 H) 3.51−3.60 (m, 1 H) 7.22 (s, 1 H) 7.57 (d, J = 2.44 Hz, 1 H) 8.17 (d, J = 7.07 Hz, 2 H) 8.70 (d, J = 7.07 Hz, 2 H) 12.70 (s, 1 H); HRMS (M + H)$^+$ calcd: 256.1444, found: 256.1450. Anal. ($C_{15}H_{17}N_3O$): C, H, N.

When required, the free base was dissolved in ethanol, treated with 4 N HCl in dioxane, and diluted with ethyl acetate until precipitation of the hydrochloride salt occurred.

The following compounds were synthesized according to the general procedure detailed above:

6-Cyclopropyl-2-pyridin-4-yl-1,5,6,7-tetrahydropyrrolo[3,2-*c*]pyridin-4-one (67). ^{1}H NMR (400 MHz, DMSO-d_6) δ ppm 0.26−0.52 (m, 4 H) 0.94−1.09 (m, 1 H) 2.78−3.08 (m, 3 H) 7.03 (d, J = 2.44 Hz, 1 H) 7.07 (d, J = 1.10 Hz, 1 H) 7.62 (d, J = 6.22 Hz, 2 H) 8.50 (d, J = 6.22 Hz, 2 H) 11.92 (s, 1 H). HRMS (M + H)$^+$ calcd 254.1288, found 254.1290. Anal. ($C_{15}H_{15}N_3O$) C: calcd 71.13, found 70.39; H: calcd 5.97, found 6.09; N: calcd 16.59, found 16.95.

7-Methyl-2-pyridin-4-yl-1,5,6,7-tetrahydropyrrolo[3,2-*c*]pyridin-4-one (77). ^{1}H NMR (400 MHz, DMSO-d_6) δ ppm 1.31 (d, J = 6.34 Hz, 3 H) 3.06−3.15 (m, 2 H) 3.45−3.52 (m, 1 H) 7.01 (d, J = 2.44 Hz, 1 H) 7.05 (bs, 1 H) 7.67 (dd, J = 6.34, 1.71 Hz, 2 H) 8.50 (dd, J = 6.22, 1.59 Hz, 2 H) 11.72 (s, 1 H). HRMS (M + H)$^+$ calcd 228.1131, found 228.1127. Anal. ($C_{13}H_{13}N_3O$): C, H, N.

7-Isopropyl-2-pyridin-4-yl-1,5,6,7-tetrahydropyrrolo[3,2-*c*]pyridin-4-one (79). A suspension of 5-isopropylpiperidine-2,4-dione **104g** (1.9 g, 12.24 mmol) and 2-bromo-1-pyridin-4-ylethanone hydrobromide (2.6 g, 9.42 mmol) in ethanol (120 mL) was treated with ammonium acetate (2.9 g, 37.7 mmol) at room temperature. The resulting solution was stirred for 16 h. The mixture was concentrated under reduced pressure, diluted with ethylacetate and washed with 0.5 N NaOH (pH = 9). The aqueous layer was extracted with ethyl acetate (×5). The collected organic layers were dried over anhydrous sodium sulfate and evaporated to dryness. The crude material was purified by flash chromatography (eluant: dichloromethane/ethanol 10:1), to give the title compound (1.4 g, 58%).

^{1}H (400 MHz, DMSO-d_6) δ ppm 0.92 (d, J = 6.95 Hz, 3 H) 0.94 (d, J = 6.70 Hz, 3 H) 1.95−2.13 (m, 1 H) 2.69 (m, 1 H) 3.35 (m, 1 H) 3.50 (m, 1 H) 6.97 (d, J = 3.61 Hz, 1 H) 7.00 (d, J = 2.43 Hz, 1 H) 7.65 (d, J = 6.22 Hz, 2 H) 8.50 (d, J = 6.22 Hz, 2 H) 11.74 (s, 1 H). HRMS (M + H)$^+$ calcd 256.1444, found 256.1447. Anal. ($C_{15}H_{17}N_3O$): C, H, N.

The following compounds were synthesized according to the general procedure detailed above:

6-Methyl-2-pyridin-4-yl-1,5,6,7-tetrahydropyrrolo[3,2-*c*]pyridin-4-one (65). ^{1}H NMR (400 MHz, DMSO-d_6) δ ppm 1.26 (d, J = 6.46 Hz, 3 H) 2.63−2.73 (dd, J = 10.00, 16.34 Hz, 1 H) 3.01 (dd, J = 16.40, 5.06 Hz, 1 H) 3.74−3.86 (m, 1 H) 7.28 (s, 1 H) 7.58 (d, J = 2.32 Hz, 1 H) 8.18 (d, J = 6.22 Hz, 2 H) 8.70 (d, J = 7.07 Hz, 2 H) 12.67 (s, 1 H). HRMS (M + H)$^+$ calcd 228.1131, found 228.1135. Anal. ($C_{13}H_{13}N_3O$): C, H, N.

6-Isobutyl-2-pyridin-4-yl-1,5,6,7-tetrahydropyrrolo[3,2-*c*]pyridin-4-one (68). ^{1}H NMR (400 MHz, DMSO-d_6) δ ppm 0.91 (dd, J = 6.58, 10.85 Hz, 6 H) 1.38 (m, 1 H) 1.53 (m, 1 H) 1.76 (m, 1 H) 2.70 (dd, J = 8.42, 16.34 Hz, 1 H) 3.05 (dd, J = 5.36, 16.34, 1 H) 3.74 (m, 1 H) 7.27 (bs, 1 H) 7.58 (d, J = 2.32 Hz, 1 H) 8.18 (d, J = 7.07 Hz, 2 H) 8.71 (d, J = 7.07 Hz, 2 H) 12.72 (bs, 1 H). HRMS (M + H)$^+$ calcd 270.1601, found 270.1595. Anal. ($C_{16}H_{19}N_3O$): C, H, N.

6,6-Dimethyl-2-pyridin-4-yl-1,5,6,7-tetrahydropyrrolo[3,2-*c*]pyridin-4-one (69). ^{1}H NMR (400 MHz DMSO-d_6) δ ppm 1.29 (s, 6 H) 2.90 (s, 2 H) 7.27 (s, 1 H) 7.59 (s, 1 H) 8.18 (d, J = 7.07 Hz, 2 H) 8.70 (d, J = 7.07 Hz, 2 H) 12.65 (bs, 1 H). HRMS (M + H)$^+$ calcd 242.1288, found 242.1297. Anal. ($C_{14}H_{15}N_3O$): C, H, N.

(*R*)-6-benzyloxymethyl-2-pyridin-4-yl-1,5,6,7-tetrahydropyrrolo[3,2-*c*]pyridin-4-one (70). ^{1}H NMR (400 MHz, DMSO-d_6) δ ppm: 2.91 (dd, J = 1.35, 16.22 Hz, 1 H) 3.01 (dd, J = 1.35, 16.22 Hz, 1 H) 3.51 (m, 2 H) 3.87 (m, 1 H) 4.53 (s, 2 H) 6.96 (bs, 1 H) 7.01 (s, 1 H) 7.34 (m, 5 H) 7.61 (d, J = 4.6 Hz, 2 H) 8.49 (d, J = 4.3 Hz, 2 H) 11.91 (bs, 1 H). HRMS (M + H)$^+$ calcd 334.1550, found 334.1555. Anal. ($C_{20}H_{19}N_3O_2$) C: calcd 72.05, found 69.92; H: calcd 5.74, found 5.96; N: calcd 12.60, found 12.22.

2-(2-Aminopyrimidin-4-yl)-6-methyl-1,5,6,7-tetrahydropyrrolo[3,2-*c*]pyridin-4-one (71). ^{1}H NMR (400 MHz, DMSO-d_6) δ ppm 1.24 (d, J = 6.34 Hz, 3 H) 2.65 (dd, J = 16.71, 10.12 Hz, 1 H) 3.01 (dd, J = 16.58, 5.00 Hz, 1 H) 3.73−3.85 (m, 1 H) 7.30 (s, 1 H) 7.31 (d, J = 7.19 Hz, 1 H) 7.52 (d, J = 2.07 Hz, 1 H) 8.03 (s, 2 H) 8.21 (d, J = 6.71 Hz, 1 H) 12.34 (s, 1 H). HRMS (M + H)$^+$ calcd 244.1193, found 244.1186. Anal. ($C_{12}H_{13}N_5O$): C, H, N.

2-(2-Aminopyrimidin-4-yl)-6-isopropyl-1,5,6,7-tetrahydropyrrolo[3,2-*c*]pyridin-4-one hydrochloride (72). ^{1}H NMR (400 MHz, DMSO-d_6) δ ppm 0.92 (dd, J = 4.15, 6.83 Hz, 6 H) 1.86 (m, 1 H) 2.79 (dd, J = 9.39, 16.95 Hz, 1 H) 2.92 (dd, J = .48, 19.90 Hz, 1 H) 3.52 (m, 1 H) 7.26 (bs, 1 H) 7.31 (d, J = 6.83 Hz, 1 H) 7.52

(bs, 1 H) 8.21 (d, $J = 6.71$ Hz, 1 H) 12.32 (bs, 1 H). HRMS (M + H)$^+$ calcd 272.1506, found 272.1501. Anal. ($C_{14}H_{15}N_3O$): C, H, N.

2-(2-Aminopyrimidin-4-yl)-6-cyclopropyl-1,5,6,7-tetrahydropyrrolo[3,2-*c*]pyridin-4-one (73). ^{1}H (400 MHz, DMSO-d_6) δ ppm 0.21−0.28 (m, 1 H) 0.30−0.36 (m, 1 H) 0.39−0.51 (m, 2 H) 0.95−1.04 (m, 1 H) 2.78−2.91 (m, 2 H) 2.97−3.05 (m, 1 H) 6.38 (bs, 2 H) 6.93 (d, $J = 5.37$ Hz, 1 H) 7.05 (d, $J = 2.07$ Hz, 1 H) 7.07 (bs, 1 H) 8.16 (d, $J = 5.24$ Hz, 1 H) 11.78 (bs, 1 H). HRMS (M + H)$^+$ calcd 270.1349, found 270.1351. Anal. ($C_{14}H_{15}N_5O$): C, H, N.

2-(2-Aminopyrimidin-4-yl)-6-isobutyl-1,5,6,7-tetrahydropyrrolo[3,2-*c*]pyridin-4-one (74). ^{1}H NMR (400 MHz, DMSO-d_6) δ ppm 0.81−0.97 (m, 6 H) 1.27−1.42 (m, 1 H) 1.42−1.58 (m, 1 H) 1.64−1.81 (m, 1 H) 2.70 (dd, $J = 16.58$, 8.41 Hz, 1 H) 3.04 (dd, $J = 16.58$, 5.24 Hz, 1 H) 3.63−3.80 (m, 1 H) 7.29 (s, 1H) 7.31 (d, $J = 6.71$ Hz, 1 H) 7.51 (s, 1 H) 8.08 (s, 2 H) 8.21 (d, $J = 6.71$ Hz, 1 H) 12.35 (s, 1 H). HRMS (M + H)$^+$ calcd 286.1662, found 286.1665. Anal. ($C_{15}H_{19}N_5O$): C, H, N.

6,6-Dimethyl-2-(2-aminopyrimidin-4-yl)-1,5,6,7-tetrahydropyrrolo[3,2-*c*]pyridin-4-one (75). ^{1}H NMR (400 MHz, DMSO-d_6) δ ppm 1.3 (m, $J = 2.7$, 0.9, 0.5 Hz, 3 H) 1.5 (m, $J = 2.7$, 0.9, 0.5 Hz, 3 H) 2.5 (m, $J = 15.6$, 1.5, 0.9, 0.5 Hz, 1 H) 2.6 (m, $J = 15.6$, 1.5, 0.9, 0.5 Hz, 1 H) 7.5 (d, $J = 0.9$ Hz, 1 H) 7.7 (d, $J = 4.8$ Hz, 1 H) 8.2 (d, $J = 4.8$ Hz, 1 H) 9.2 (m, 1 H). HRMS (M + H)$^+$ calcd 258.1349, found 258.1356. Anal. ($C_{13}H_{15}N_5O$): C, H, N.

***(R)*-2-(2-Aminopyrimidin-4-yl)-6-benzyloxymethyl-1,5,6,7-tetrahydropyrrolo[3,2-*c*]pyridin-4-one (76).** ^{1}H (400 MHz, DMSO-d_6) δ ppm 2.88 (dd, $J = 7.32$, 16.71 Hz, 1 H), 2.97 (dd, $J = 5.90$, 16.71 Hz, 1 H), 3.46 (m, 2 H), 3.82 (m, 1 H), 4.49 (s, 2 H), 6.28 (bs, 2 H), 6.87 (d, $J = 5.24$ Hz, 1 H), 6.93 (m, 1 H), 6.99 (s, 1 H), 7.30 (m, 5 H), 8.13 (d, $J = 5.24$ Hz, 1 H), 11.74 (bs, 1 H). HRMS (M + H)$^+$ calcd 350.1611, found 350.1614. Anal. ($C_{19}H_{19}N_5O_2$): C, H, N.

7-Ethyl-2-pyridin-4-yl-1,5,6,7-tetrahydropyrrolo[3,2-*c*]pyridin-4-one (78). ^{1}H NMR (400 MHz, DMSO-d_6) δ ppm 0.96 (t, $J = 7.44$ Hz, 3 H) 1.59 (m, 1 H) 1.82 (m, 1 H) 2.86 (m, 1 H) 3.21(m, 1 H) 3.53 (m, 1 H) 7.00 (s, 1 H) 7.01 (s, 1 H) 7.65 (m, 2 H) 8.49 (m, 2 H) 11.75 (s, 1 H). HRMS (M + H)$^+$ calcd 242.1288, found 242.1291. Anal. ($C_{14}H_{15}N_3O$): C, H, N.

7-Cyclobutyl-2-pyridin-4-yl-1,5,6,7-tetrahydropyrrolo[3,2-*c*]pyridin-4-one (80). ^{1}H (400 MHz, DMSO-d_6) δ ppm 1.75−1.87 (m, 4 H) 2.00−2.08 (m, 2 H) 2.55−2.64 (m, 1 H) 2.88−2.94 (m, 1 H) 3.18−3.23 (m, 1 H) 3.54 (dd, $J = 12.62$, 4.82 Hz, 1 H) 7.18 (bd, $J = 4.39$ Hz, 1 H) 7.55 (d, $J = 2.19$ Hz, 1 H) 8.20 (d, $J = 7.07$ Hz, 2 H) 8.70 (d, $J = 6.95$ Hz, 2 H) 12.46 (bs, 1 H). HRMS (M + H)$^+$ calcd 268.1444, found 268.1440. Anal. ($C_{16}H_{17}N_3O$): C, H, N.

7-(2-Fluoroethyl)-2-pyridin-4-yl-1,5,6,7-tetrahydropyrrolo[3,2-*c*]pyridin-4-one (81). ^{1}H (400 MHz, DMSO-d_6) δ ppm 1.92 (m, 1 H) 2.19 (m, 1 H) 3.10 (m, 1 H) 3.26 (m, 1 H) 3.53 (m, 1 H) 4.54 (m, 1 H) 4.63 (m, 1 H) 7.01 (d, $J = 2.29$ Hz, 1 H) 7.07 (s, 1 H) 7.65 (d, $J = 6.12$ Hz, 2 H) 8.49 (d, $J = 6.12$ Hz, 2 H) 11.80 (s, 1 H). HRMS (M + H)$^+$ calcd 260.1194, found 260.1199. Anal. ($C_{14}H_{14}FN_3O$): C, H, N.

7,7-Dimethyl-2-pyridin-4-yl-1,5,6,7-tetrahydropyrrolo[3,2-*c*]pyridin-4-one (82). ^{1}H (400 MHz, DMSO-d_6) δ ppm 1.38 (s, 6 H) 3.20 (s, 2 H) 7.37 (s, 1 H) 7.56 (d, $J = 2.32$ Hz, 1 H) 8.36 (d, $J = 6.95$ Hz, 2 H) 8.72 (d, $J = 6.95$ Hz, 2 H) 12.34 (s, 1 H). HRMS (M + H)$^+$ calcd 242.1288, found 242.1287. Anal. ($C_{14}H_{15}N_3O$): C, H, N.

7,7-Diethyl-2-pyridin-4-yl-1,5,6,7-tetrahydropyrrolo[3,2-*c*]pyridin-4-one (83). ^{1}H NMR (400 MHz, DMSO-d_6) δ ppm 0.83 (t, $J = 7.50$ Hz, 6 H) 1.70−1.88 (m, 4 H) 3.28 (d, $J = 2.44$ Hz, 2 H) 7.31 (bs, 1 H) 7.59 (d, $J = 2.32$ Hz, 1 H) 8.32 (d, $J = 6.71$ Hz, 2 H) 8.72 (d, $J = 7.07$ Hz, 2 H) 11.99 (bs, 1 H). HRMS (M + H)$^+$ calcd 270.1601, found 270.1602. Anal. ($C_{16}H_{19}N_3O$): C, H, N.

7-Phenyl-2-pyridin-4-yl-1,5,6,7-tetrahydropyrrolo[3,2-*c*]pyridin-4-one (84). ^{1}H (400 MHz, DMSO-d_6) δ 3.87 (ddd, $J = 12.71$, 5.46, 0.98 Hz, 1 H) 4.42 (t, $J = 4.51$ Hz, 1 H) 7.17−7.22 (m, 2 H) 7.26−7.40 (m, 4 H) 7.69 (d, $J = 2.44$ Hz, 1 H) 8.22 (d, $J = 7.07$ Hz, 2 H) 8.72 (d, $J = 6.95$ Hz, 2 H) 12.59 (bs, 1 H). HRMS (M + H)$^+$ calcd 290.1288, found 290.1291. Anal. ($C_{18}H_{15}N_3O$) H; C: calcd 74.72, found, 75.79; N: calcd 14.52, found 13.98.

2-(2-Aminopyrimidin-4-yl)-7-methyl-1,5,6,7-tetrahydropyrrolo[3,2-*c*]pyridin-4-one (85). ^{1}H NMR (400 MHz, DMSO-d_6) δ ppm 1.29 (d, $J = 6.58$ Hz, 3 H) 3.06−3.24 (m, 2 H) 3.41−3.56 (m, 1 H) 7.30 (s, 1 H) 7.35 (d, $J = 6.83$ Hz, 1 H) 7.51 (s, 1 H) 8.03 (s, 2 H) 8.23 (d, $J = 6.71$ Hz, 1 H) 12.24 (s, 1 H). HRMS (M + H)$^+$ calcd 244.1193, found 244.1189. Anal. ($C_{12}H_{13}N_5O$): C, H, N.

2-(2-Aminopyrimidin-4-yl)-7-ethyl-1,5,6,7-tetrahydropyrrolo[3,2-*c*]pyridin-4-one (86). ^{1}H NMR (400 MHz, DMSO-d_6) δ ppm 0.94 (t, $J = 6.95$ Hz, 3 H) 1.7 (m, 2 H) 2.9 (m, 1 H) 3.3 (m, 2 H) 7.25 (bs, 1 H) 7.35 (d, $J = 6.83$ Hz, 1 H) 7.5 (s, 1 H) 8.04 (bs, 2 H) 8.22 (d, $J = 6.83$ Hz, 1 H) 12.25 (bs, 1 H). HRMS (M + H)$^+$ calcd 258.1349, found 258.1350. Anal. ($C_{13}H_{15}N_5O$): C, H, N.

The racemate was subjected to separation by chiral chromatography on a Chiralpack AS column (5 cm × 50 cm). Mobile phase: *n*-hexane/isopropanyl alcohol/ethanol/methanol 3:3:3:1. First eluted peak (**86**−**1**): ee 98.5%, second eluted peak (**86**−**2**): ee 97%.

2-(2-Aminopyrimidin-4-yl)-7-isopropyl-1,5,6,7-tetrahydropyrrolo[3,2-*c*]pyridin-4-one (87). ^{1}H (400 MHz, DMSO-d_6) δ ppm 0.91 (t, $J = 6.95$ Hz, 6 H) 1.07 (t, $J = 6.95$ Hz, 1 H) 1.96−2.10 (m, 1 H) 2.66−2.74 (m, 1 H) 3.40−3.54 (m, 1 H) 6.28−6.39 (m, 2 H) 6.95 (d, $J = 5.37$ Hz, 1 H) 6.97 (s, 1 H) 7.03 (d, $J = 2.19$ Hz, 1 H) 8.16 (d, $J = 5.24$ Hz, 1 H) 11.64 (s, 1 H). HRMS (M + H)$^+$ calcd 272.1506, found 272.1512. Anal. ($C_{14}H_{17}N_5O$): C, H, N.

The racemate was subjected to separation by chiral chromatography on a Chiralpack AS column (5 cm × 50 cm). Mobile phase: *n*-hexane/isopropyl alcohol/ethanol/methanol 3:3:3:1. First eluted peak (**87**−**1**): ee 99%, second eluted peak (**87**−**2**): ee 99%.

2-(2-Aminopyrimidin-4-yl)-7-cyclobutyl-1,5,6,7-tetrahydropyrrolo[3,2-*c*]pyridin-4-one (88). ^{1}H (400 MHz, DMSO-d_6) δ ppm 1.71−1.85 (m, 4 H) 1.99−2.10 (m, 2 H) 2.50−2.61 (m, 1 H) 2.94 (dd, $J = 9.27$, 3.66 Hz, 1 H) 3.14−3.21 (m, 1 H) 3.51 (dd, $J = 12.74$, 4.82 Hz, 1 H) 7.19 (d, $J = 4.15$ Hz, 1 H) 7.34 (d, $J = 6.58$ Hz, 1 H) 7.48 (d, $J = 2.07$ Hz, 1 H) 7.97 (bs, 3 H) 8.24 (d, $J = 6.71$ Hz, 1 H) 12.26 (bs, 1 H). HRMS (M + H)$^+$ calcd 284.1506, found 284.1506. Anal. ($C_{15}H_{17}N_5O.0.5\ H_2O$): C, H, N.

The racemate was subjected to separation by chiral chromatography on a Chiralpack AS column (5 cm × 50 cm). Mobile phase: *n*-hexane/ethanol/methanol 55:30:15. First eluted peak (**88**−**1**) ee 99%, second eluted peak (**88**−**2**): ee 97%.

2-(2-Aminopyrimidin-4-yl)-7-(2-fluoroethyl)-1,5,6,7-tetrahydropyrrolo[3,2-*c*]pyridin-4-one (89). ^{1}H (400 MHz, DMSO-d_6) δ ppm 1.92 (m, 1 H), 2.15 (m, 1 H), 3.11 (m, 1 H), 3.32 (m, 1 H), 3.52 (dd, $J = 5.12$ Hz, $J = 12.33$ Hz, 1 H), 4.52 (t, $J = 6.04$ Hz, 1 H), 4.64 (t, $J = 6.04$ Hz, 1 H), 6.33 (s, 2 H), 6.94 (d, $J = 5.31$ Hz, 1 H), 7.04 (s, 1 H), 7.07 (s, 1 H), 8.17 (d, $J = 5.31$ Hz, 1 H), 11.68 (s, 1 H). HRMS (M + H)$^+$ calcd 276.1255, found 276.1258. Anal. ($C_{13}H_{14}FN_5O$): C, H, N.

The racemate was subjected to separation by chiral column chromatographyc on a Chiralcell OJ column and eluting with *n*-hexane/ethanol/methanol 60:35:5. (*S*)-isomer, first eluted peak: ee 99%, (*R*)-isomer: second eluted peak: ee 96%.

2-(2-Aminopyrimidin-4-yl)-7,7-dimethyl-1,5,6,7-tetrahydropyrrolo[3,2-*c*]pyridin-4-one (90). ^{1}H (500 MHz, DMSO-d_6) δ ppm 1.37 (s, 6 H) 3.20 (s, 2 H) 7.39−7.43 (m, 1 H) 7.46 (d, $J = 6.70$ Hz, 1 H) 7.52 (s, 1 H) 8.16 (s, 2 H) 8.28 (d, $J = 6.70$ Hz, 1 H) 12.20 (s, 1 H). HRMS (M + H)$^+$ calcd 258.1349, found 258.1349. Anal. ($C_{13}H_{15}N_5O$): C, H, N.

2-(2-Aminopyrimidin-4-yl)-7,7-diethyl-1,5,6,7-tetrahydropyrrolo[3,2-*c*]pyridin-4-one (91). ^{1}H NMR (400 MHz, DMSO-d_6) δ ppm 0.80 (t, $J = 7.44$ Hz, 6 H) 1.73−1.85 (m, 4 H) 3.27 (d, $J = 2.56$ Hz, 2 H) 7.31 (s, 1 H) 7.37−7.43 (m, 1 H) 7.46 (s, 1 H) 7.91 (s, 2 H) 8.24 (d, $J = 6.58$ Hz, 1 H) 11.98 (s, 1 H). HRMS (M + H)$^+$ calcd 286.1662, found 286.1658. Anal. ($C_{15}H_{19}N_5O$) C: calcd 55.99, found 50.51; H: calcd 6.26, found 6.21; N: calcd 21.76, found 19.65.

2-(2-Aminopyrimidin-4-yl)-7-phenyl-1,5,6,7-tetrahydropyrrolo[3,2-*c*]pyridin-4-one (92). ^{1}H NMR (400 MHz, DMSO-d_6) δ ppm 3.7 (m, $J = 13.0$, 8.0, 4.0 Hz, 1 H) 3.8 (m, $J = 8.0$, 6.0, 1.5, 0.9, 0.6 Hz, 1 H) 3.9 (m, $J = 13.0$, 6.0, 3.0 Hz, 1 H) 7.0 (m, $J = 7.3$, 7.1,

1.4, 1.0 Hz, 1 H) 7.0 (m, J = 7.3, 7.1, 1.4, 1.0 Hz, 1 H) 7.2 (m, J = 7.1, 1.2 Hz, 1 H) 7.4 (m, J = 7.3, 1.2, 1.2, 1.0, 0.6 Hz, 1 H) 7.4 (m, J = 7.3, 1.2, 1.2, 1.0, 0.6 Hz, 1 H) 7.5 (d, J = 0.9 Hz, 1 H) 7.7 (d, J = 4.8 Hz, 1 H) 8.2 (d, J = 4.8 Hz, 1 H) 9.2 (s, 1 H). HRMS $(M + H)^+$ calcd 306.1349, found 306.1346. Anal. ($C_{17}H_{15}N_5O$): C, H, N.

2-(2-Aminopyrimidin-4-yl)-7-(3,3,3-trifluoropropyl)-1,5,6,7-tetrahydropyrrolo[3,2-*c*]pyridin-4-one (93). ^{1}H (400 MHz, DMSO-d_6) δ ppm 1.78 (m, 1 H) 2.01 (m, 1 H) 2.27 (m, 1 H) 2.45 (m, 1 H) 3.03 (m, 1 H) 3.26 (m, 1 H) 3.58 (m, 1 H) 6.33 (s, 2 H) 6.96 (d, J = 5.22 Hz, 1 H) 7.05 (d, J = 2.24 Hz, 1 H) 7.07 (d, J = 2.58 Hz, 1 H) 8.17 (d, J = 5.22 Hz, 1 H) 11.78 (s, 1 H). HRMS $(M + H)^+$ calcd 326.1223, found 326.1221. Anal. ($C_{14}H_{14}F_3N_5O$) C: calcd 51.69, found, 51.14; H: calcd 4.34, found 4.67; N; F: calcd 17.50, found 16.98; N: calcd 21.53, found 21.24.

The racemate was subjected to separation by chiral chromatography on a Chiralcell OD column, eluting with *n*-hexane/ethanol 75:25. First eluted peak (**93**−**1**): ee 99%, second eluted peak (**93**−**2**): ee 98%.

2-(2-Aminopyrimidin-4-yl)-7-(2-benzyloxyethyl)-1,5,6,7-tetrahydropyrrolo[3,2-*c*]pyridin-4-one (94). ^{1}H NMR (400 MHz, DMSO-d_6) δ ppm 1.80 (m, 1 H) 2.07 (m, 1 H) 3.07 (m, 1 H) 3.24 (m, 1 H) 3.47 (m, 1 H) 3.55 (m, 2 H) 4.50 (m, 2 H) 6.30 (s, 2 H) 6.91 (d, J = 5.30 Hz, 1 H) 7.01 (s, 1 H) 7.03 (s, 1 H) 7.25−7.35 (m, 5 H) 8.14 (d, J = 5.30 Hz, 1 H) 11.60 (s, 1 H). HRMS $(M + H)^+$ calcd 364.1768, found 364.1773. Anal. ($C_{20}H_{21}N_5O_2$): C, H, N.

2-(2-Aminopyrimidin-4-yl)-7-(3-benzyloxypropyl)-1,5,6,7-tetrahydropyrrolo[3,2-*c*]pyridin-4-one (95). ^{1}H (400 MHz, DMSO-d_6) δ ppm 1.45−1.80 (m, 4 H) 2.92 (m, 1 H) 3.19 (m, 1 H) 3.42 (t, J = 5.98 Hz, 2 H) 3.49 (m, 1 H) 4.43 (s, 2 H) 6.29 (s, 2 H) 6.90 (d, J = 5.21 Hz, 1 H) 6.99 (m, 2 H) 7.20 − 7.35 (m, 5 H) 8.13 (d, J = 5.21 Hz, 1 H) 11.62 (s, 1 H). HRMS $(M + H)^+$ calcd 378.1924, found 378.1913. Anal. ($C_{21}H_{23}N_5O_2$) H; C: calcd 66.83, found 65.12; N: calcd 18.55, found 17.76.

2-(2-Aminopyrimidin-4-yl)-7-(2-hydroxyethyl)-1,5,6,7-tetrahydropyrrolo[3,2-*c*]pyridin-4-one (96). To a solution of 2-(2-amino-pyrimidin-4-yl)-7-(2-benzyloxy-ethyl)-1,5,6,7-tetrahydropyrrolo[3,2-*c*]pyridin-4-one **94** (1.55 g, 4.2 mmol) in ethanol (150 mL), 10% Pd on carbon (0.35 g) and cyclohexene (150 mL) were added and the mixture was refluxed for 18 h. Two more additions of 10% Pd on carbon (150 mg each) were done until completion of the reaction (2 days). After filtration and concentration, the title compound was obtained (1.15 g, 98% yield).

^{1}H NMR (400 MHz, DMSO-d_6) δ ppm 1.80 (m, 1 H), 2.07 (m, 1 H), 3.07 (m, 1 H), 3.24 (m, 1 H), 3.47 (m, 1 H), 3.55 (m, 2 H), 4.50 (m, 2 H), 6.30 (s, 2 H), 6.91 (d, J = 5.24 Hz, 1 H), 7.01 (s, 1 H), 7.03 (s, 1 H), 7.25−7.35 (m, 5 H), 8.14 (d, J = 5.24 Hz, 1 H), 11.60 (s, 1 H). HRMS $(M + H)^+$ calcd 274.1298, found 274.1291. Anal. ($C_{13}H_{15}N_5O_2$.0.7 H_2O): C, H, N.

2-(2-Aminopyrimidin-4-yl)-7-(3-hydroxypropyl)-1,5,6,7-tetrahydropyrrolo[3,2-*c*]pyridin-4-one (97). To a cold (−78 °C) solution of 2-(2-amino-pyrimidin-4-yl)-7-(3-benzyloxy-propyl)-1,5,6,7-tetrahydro-pyrrolo[3,2-*c*]pyridin-4-one **95** (0.26 g, 0.69 mmol) in anhydrous dichloromethane (20 mL), 1 M boron trichloride in dichloromethane (4.2 mL, 4 mmol) was added dropwise under stirring and the mixture was maintained at −78 °C for 3 h. More 1 M boron trichloride in dichloromethane (1 mL) was added, and after 1 h, methanol (5 mL) and dichloromethane (5 mL) were added. After solvent evaporation the residue was taken up in methanol (15 mL), sodium bicarbonate (0.5 g) was added and the mixture was stirred for 2 h at room temperature. After filtration and concentration, the residue was purified by flash chromatography (eluant:dichloromethane/methanol 20:1, then 10:1). Obtained the title compound (0.21 g, 90% yield).

^{1}H (400 MHz, DMSO-d_6) δ ppm 1.40 (m, 1 H), 1.54 (m, 2 H), 1.65 (m, 1 H), 2.91 (m, 1 H), 3.18 (m, 1 H), 3.40 (m, 2 H), 3.48 (m, 1 H), 4.44 (t, J = 5.12 Hz, 1 H), 6.30 (s, 2 H), 6.91 (d, J = 5.25 Hz, 1 H), 6.99 (s, 1 H), 7.02 (s, 1 H), 8.13 (d, J = 5.25 Hz1 H), 11.62 (s, 1 H). HRMS $(M + H)^+$ calcd 288.1455, found 288.1455. Anal. ($C_{14}H_{17}N_5O_2$): C, H, N.

2-Methyl-4,6-dioxo-piperidine-1-carboxylic Acid *tert*-Butyl Ester (100a). To a solution of 3-(*tert*-butoxycarbonylamino)butanoic acid (26.8 g, 132 mmol), 2,2-dimethyl-1,3-dioxane-4,6-dione (20.9 g, 145 mmol) and 4-dimethylaminopyridine (24.2 g, 198 mmol) in anhydrous dichloromethane (700 mL) at 0 °C, 1-(3-dimethylaminopropyl)-3-ethylcarbodiimide hydrochloride (30.4 g, 158 mmol) was added and the resulting solution was stirred overnight at room temperature. The reaction mixture was washed (500 mL × 4) with 5% aqueous potassium bisulfate. The organic layer was dried over anhydrous sodium sulfate, filtered, and concentrated, affording crude [3-(2,2-dimethyl-4,6-dioxo-[1,3]dioxan-5-yl)-1-methyl-3-oxo-propyl]-carbamic acid *tert*-butyl ester that was dissolved in 600 mL of ethyl acetate and refluxed for 4 h. The volume was reduced to 150 mL and the resulting solution was allowed to crystallize at 4 °C overnight. The solid was filtered and washed with cold ethyl acetate, affording the title compound (19.5 g, 65% yield).

^{1}H (300 MHz, DMSO-d_6) δ ppm 1.36 (d, J = 6.50 Hz, 3 H) 1.41 (s, 9 H) 2.63 (d, J = 6.03 Hz, 2 H) 3.01 (s, 2 H) 4.32 (m, 1 H). ESI (+) MS: m/z 228 (MH^+).

Optionally, the *t*-butoxycarbonyl group can be removed by acidic treatment (4 N HCl in dioxane or tetrahydrofuran) at room temperature to yield **104a**.

The following compounds were synthesized according to the general procedure detailed above:

6-Isopropylpiperidine-2,4-dione (104b). ^{1}H NMR (400 MHz, DMSO-d_6) δ ppm 0.84 (d, J = 6.88 Hz, 3 H) 0.93 (d, J = 6.88 Hz, 3 H) 2.17 (m, 1 H) 2.21 (m, 2 H) 3.23 (s, 2H) 3.45 (m, 1H) 7.95 (s, 1 H). ESI (+) MS: m/z 156 (MH^+).

2-Isobutyl-4,6-dioxo-piperidine-1-carboxylic Acid *tert*-Butyl Ester (100c). ^{1}H (300 MHz, DMSO-d_6) δ ppm 0.91 (d, J = 6.60 Hz, 6 H) 1.25−1.34 (m, 1 H) 1.40 (s, 9 H) 1.81−1.90 (m, 2 H) 2.75 (d, J = 5.94 Hz, 2 H) 3.22 (s, 2 H) 4.69 (m, 1 H). ESI (+) MS: m/z 270 (MH^+).

(*R*)-6-Benzyloxymethyl-piperidine-2,4-dione (104d). ^{1}H NMR (400 MHz, DMSO-d_6) δ ppm: 2.4 (dd, 1 H) 2.7 (dd, 1 H) 3.01−3.17 (dd, 2 H) 3.48 (s, 2 H) 3.77 (m, 1 H) 4.46 (s, 2 H) 7.28 (m, 2 H) 7.33 (m, 3 H) 8.06 (bs, 1 H). ESI (+) MS: m/z 234 (MH^+).

2-Cyclopropyl-4,6-dioxo-piperidine-1-carboxylic Acid *tert*-Butyl Ester (100e). ^{1}H (300 MHz, DMSO-d_6) δ ppm 0.39−0.57 (m, 4 H) 1.10−1.25 (m, 1 H) 1.39−1.44 (s, 9 H) 2.25 (dd, J = 17.44, 1.10 Hz, 1 H) 2.89 (ddd, J = 17.50, 6.34, 1.77 Hz, 1 H) 3.67 (ddd, J = 9.36, 6.37, 1.10 Hz, 1 H) 4.99 (d, J = 1.95 Hz, 1 H) 11.13 (s, 1 H). ESI (+) MS: m/z 254 (MH^+).

Ethyl 3-amino-3-methylbutanoate Hydrochloride (101f). A solution of commercial ethyl 3-methylbut-2-enoate (1 g, 7.8 mmol) in absolute ethanol (12 mL) was cooled to −20 °C and saturated with gaseous ammonia. The tube was sealed and kept at 90 °C for 24 h. The reaction was cooled to room temperature, bubbled with nitrogen to eliminate the residual ammonia and treated with a 4 N solution of HCl in dioxane (1.9 mL). After 30 min stirring, the mixture was evaporated under reduced pressure to give ethyl 3-amino-3-methylbutanoate hydrochloride as a gray solid (1.19 g, 84%).

^{1}H (400 MHz, DMSO-d_6) δ ppm 1.2 (t, 3 H) 1.26 (s, 6 H) 2.65 (s, 2 H) 4.1 (q, 2 H) 8.27 (bs, 3 H). ESI (+) MS: m/z 146 (MH^+).

Ethyl 2-(aminomethyl)-3-methylbutanoate Hydrochloride (101g). To a solution of commercial ethyl 2-cyano-3-methylbut-2-enoate (5.0 g, 32.6 mmol) absolute ethanol (300 mL), 700 mg of PtO_2 and 12 mL of 4 N HCl were added. The reaction mixture was hydrogenated at room temperature for 5 h (30 psi). Filtration on celite and evaporation of the solvent afforded the title compound (6.4 g, quantitative yield).

^{1}H (400 MHz, DMSO-d_6) δ ppm 0.90 (d, J = 6.83 Hz, 3 H) 0.93 (d, J = 6.83 Hz, 3 H) 1.24 (t, J = 7.13 Hz, 3 H) 1.92−2.06 (m, 1 H) 2.53−2.60 (m, 1 H) 2.84−3.17 (m, 2 H) 4.05−4.24 (m, 2 H) 7.84 (s, 3 H). ESI (+) MS: m/z 160 (MH^+).

2-Aminomethyl-2-ethyl-butyric Acid Ethyl Ester Hydrochloride (101j). A mixture of commercial 2-cyano-2-ethyl-butyric acid ethyl ester (5 g, 29.8 mmol), PtO_2 (640 mg, 29.8 mmol), absolute ethanol (290 mL), and 4 N HCl in dioxane (13 mL) was hydrogenated at 30 psi of hydrogen in a Parr apparatus for 5 h at room temperature.

After filtration through celite and solvent evaporation, the title compound was obtained as a white crystalline solid (5 g, 82% yield).

^{1}H (400 MHz, DMSO-d_6) δ ppm 0.79 (t, J = 7.44 Hz, 6 H) 1.25 (t, J = 7.07 Hz, 3 H) 1.62 (q, J = 7.48 Hz, 4 H) 2.99 (q, J = 5.69 Hz, 2 H) 4.15 (q, J = 7.07 Hz, 2 H) 7.81 (bs, 3 H). ESI (+) MS: m/z 174 (MH^+).

3-Amino-2-cyclobutyl-propionic Acid Ethyl Ester (101l). A mixture of ethyl cyanoacetate (0.73 g, 6.48 mmol), cyclobutanone (0.5 g, 7.1 mmol), ammonium acetate (0.05 g, 0.65 mmol), and glacial acetic acid (0.08 g, 1.3 mmol) in toluene (2.2 mL) was refluxed for 4 h using a Dean−Stark water separator. The mixture was washed with water, dried over anhydrous sodium sulfate, and concentrated to yield crude cyano-cyclobutylidene-acetic acid ethyl ester (0.9 g, 84%).

^{1}H (500 MHz, DMSO-d_6) δ ppm 1.20−1.25 (m, 3 H) 2.10−2.17 (m, 2 H) 3.09 (t, J = 7.79 Hz, 2 H) 3.24 (t, J = 7.79 Hz, 2 H) 4.16 (q, J = 7.18 Hz, 1 H) 4.19 (q, J = 7.08 Hz, 1 H).

The crude ester was hydrogenated with PtO_2 (0.12 g, 5.6 mmol) in absolute ethanol (55 mL) and 4 N HCl in dioxane (10 mL) at 50 psi of hydrogen in a Parr apparatus for 4 h at room temperature. After filtration through celite and solvent evaporation, the title compound was obtained (0.95 g, 84% yield).

^{1}H (500 MHz, DMSO-d_6) δ ppm 1.18 (t, J = 7.03 Hz, 3 H) 1.63−1.82 (m, 4 H) 1.83−1.94 (m, 1 H) 1.95−2.04 (m, 1 H) 2.31−2.42 (m, 1 H) 2.63−2.69 (m, 2 H) 2.81−3.01 (m, 1 H) 4.01−4.19 (m, 2 H) 8.10−8.24 (bs, 3 H). ESI (+) MS: m/z 172 (MH^+).

6,6-Dimethyl-2,4-dioxopiperidine (104f). Ethyl 3-amino-3-methylbutanoate hydrochloride **101f** (0.87 g, 4.79 mmol) was suspended in dichloromethane (12 mL) and triethylamine (1.4 mL, 10 mmol). The mixture was cooled to 0 °C and treated dropwise with ethyl 3-chloro-3-oxopropanoate (0.64 mL, 5 mmol). The reaction was stirred at room temperature for 2 h, diluted with dichloromethane, washed with 1 N HCl and then with 5% aqueous sodium bicarbonate, dried over anhydrous sodium sulfate, and evaporated to dryness to yield ethyl 3-[(3-ethoxy-3-oxopropanoyl)amino]-3-methylbutanoate (**102f**, 1.2 g, 97% yield) as a red oil.

^{1}H (300 MHz, DMSO-d_6) δ ppm 1.11−1.21 (m, 6 H) 1.29 (s, 6 H) 2.71 (s, 2 H) 3.14 (s, 2 H) 3.95−4.15 (m, 4 H) 7.75 (bs, 1 H).

To a solution of sodium ethoxide, obtained from sodium metal (0.12 g, 5.55 mmol) in anhydrous ethanol (7 mL), a solution of **102f** (1.2 g, 4.62 mmol) in dry toluene (7 mL) was added dropwise at room temperature, with stirring. The reaction mixture was heated at 80 °C for 2 h and then it was concentrated to reduced volume and the residue was dissolved in toluene (15 mL). The organic phase was extracted with water (40 mL), the aqueous phase was acidified to pH 2−3 with 1 N HCl and extracted with ethyl acetate (4 × 50 mL). The organic phase was washed with brine, dried over anhydrous sodium sulfate, and concentrated to give ethyl 6,6-dimethyl-2,4-dioxopiperidine-3-carboxylate **103f** as a yellow solid (0.7 g, 71% yield), which was dissolved in acetonitrile containing 1% of water (15 mL) and refluxed for 2 h. After evaporating to dryness, the crude material was suspended in isopropyl ether, kept under vigorous stirring, and filtered to give the title compound (0.39 g, 85% yield) as a light-brown solid.

^{1}H (300 MHz, DMSO-d_6) δ ppm 1.18 (s, 6 H) 2.49 (bs, 2 H) 3.13 (bs, 2 H) 8.13 (bs, 1 H). ESI (+) MS: m/z 142 (MH^+).

The following compounds were synthesized according to the general procedure detailed above:

5-Isopropylpiperidine-2,4-dione (104g). ^{1}H NMR (400 MHz, DMSO-d_6) δ ppm 0.85 (d, J = 6.83 Hz, 3 H) 0.94 (d, J = 6.95 Hz, 3 H) 2.07−2.17 (m, 1 H) 2.25−2.33 (m, 1 H) 3.09−3.41 (m, 4 H) 8.03 (s, 1 H). ESI (+) MS: m/z 156 (MH^+).

5-Methylpiperidine-2,4-dione (104h). ^{1}H NMR (400 MHz, DMSO-d_6) δ ppm 1.09 (d, J = 6.95 Hz, 3 H) 2.49−2.59 (m, 1 H) 3.49−3.57 (m, 1 H) 3.68−3.77 (m, 1 H) 4.92 (s, 1 H) 11.17 (s, 1 H). ESI (+) MS: m/z 128 (MH^+).

5,5-Dimethylpiperidine-2,4-dione (104k). ^{1}H NMR (300 MHz, DMSO-d_6) δ ppm 1.0 (s, 6 H) 3.15 (s, 2 H) 3.25 (s, 2 H) 8.0 (s, 1 H). ESI (+) MS: m/z 142 (MH^+).

5-Phenylpiperidine-2,4-dione (104i). ^{1}H NMR (300 MHz, DMSO-d_6) δ ppm 3.25 (d, J = 18.75 Hz, 1 H) 3.42−3.70 (m, 2 H), 3.61 (d, J = 18.75 Hz, 1 H) 3.81 (dd, J = 5.57, 9.67 Hz, 1 H) 7.26 (m, 5 H) 8.20 (bs, 1 H). ESI (+) MS: m/z 190 (MH^+).

5,5-Diethylpiperidine-2,4-dione (104j). ^{1}H NMR (400 MHz, DMSO-d_6) δ ppm 0.77 (t, J = 7.56 Hz, 6 H) 1.46 (q, J = 7.68 Hz, 4 H) 3.23 (d, J = 3.78 Hz, 2 H) 3.26 (s, 2 H) 7.98 (s, 1 H). ESI (+) MS: m/z 170 (MH^+).

5-Cyclobutylpiperidine-2,4-dione (104l). ^{1}H (400 MHz, DMSO-d_6) δ ppm 1.68−1.87 (m, 4 H) 1.87−1.96 (m, 1 H) 1.95−2.03 (m, 1 H) 2.40−2.52 (m, 2 H) 2.98−3.05 (m, 1 H) 3.16 (d, J = 1.71 Hz, 2 H) 3.23−3.34 (m, 1 H) 7.96 (bs, 1 H). ESI (+) MS: m/z 168 (MH^+).

The preparation of **104m**,**p**,**q** is reported in the literature.[24]

5-(2-Fluoroethyl)-piperidine-2,4-dione (104n). To a solution of *tert*-butyl 2,4-dioxopiperidine-1-carboxylate (7.7 g, 36.1 mmol) in dry tetrahydrofuran (180 mL), cooled to −30 °C under nitrogen, lithium bis(trimethylsilyl)amide (108 mL of 1 M solution in tetrahydrofuran) was added dropwise. After 20 min stirring, 1-bromo-2-fluoro ethane (10 mL, 135.3 mmol) was added and the solution was stirred at −30 °C for 1 h. The reaction mixture was poured into 5% aqueous potassium bisulfate and extracted with dichloromethane (300 mL × 2). The organic layers were joined, dried over anhydrous Na_2SO_4. and filtered. Trifluoroacetic acid (75 mL) was added, and the resulting solution was stirred at room temperature for 1 h. After evaporation, the residue was purified by flash chromatography (dichloromethane/ethanol 100:2, then 100:4), thereby obtaining the title product as a white solid (3 g, 52%).

^{1}H (400 MHz, DMSO-d_6) δ ppm 1.65 (m, 1 H) 2.07 (m, 1 H) 2.63 (m, 1 H) 3.15−3.43 (m, 4 H) 4.48 (m, 1 H) 4.52 (m, 1 H) 8.08 (s, 1 H). ESI (+) MS: m/z 160 (MH^+).

The following compound was synthesized according to the general procedure detailed above:

5-(3,3,3-Trifluoropropyl)-piperidine-2,4-dione (104o). from 1-trifluoro-3-iodo-propane.

^{1}H (400 MHz, DMSO-d_6) δ ppm 1.82 (m, 1 H) 2.12 (m, 1 H) 2.25 (m, 1 H) 2.44 (m, 1 H) 3.13−3.43 (m, 5 H) 8.05 (s, 1 H). ESI (+) MS: m/z 210 (MH^+).

Ethyl-5-[(*tert*-butoxycarbonyl)amino]-6-methyl-3-oxoheptanoate (105b). 3-[(*tert*-Butoxycarbonyl)amino]-4-methylpentanoic acid **98b** (1 g, 4.33 mmol) and 1,1′-carbonyldiimidazole (1.04 g, 6.4 mmol) in anhydrous tetrahydrofuran (9 mL) was left shaking at room temperature for 3 h. Then, 0.817 g of magnesium chloride, 1.45 g of potassium ethylmalonate, and 16 mL of anhydrous tetrahydrofuran were added. The temperature was brought to 48 °C and the suspension left shaking overnight then filtered. The solvent was removed, the raw product was dissolved in ethyl acetate, washed with 5% aqueous sodium bisulfate (×3), with 5% aqueous sodium bicarbonate (×3), with brine, dried over anhydrous sodium sulfate, and concentrated. The raw product was purified by flash chromatography (eluant:toluene/ethyl acetate 85:15), thereby affording the title compound (1.06 g, 81%).

^{1}H (400 MHz, DMSO-d_6) δ ppm 0.8 (d, 6 H) 1.17 (t, 3 H) 1.38 (s, 9 H) 1.57−1.69 (m, 1 H) 2.45−2.65 (m, 2 H) 3.59 (s, 2 H) 3.67−3.77 (m, 1 H) 4.10 (q, J = 7.07 Hz, 2 H) 6.68 (d, J = 8.78 Hz, 1 H).

The following compound was synthesized according to the general procedure detailed above:

Ethyl-5-[(*tert*-butoxycarbonyl)amino]-5-cyclopropyl-3-oxopentanoate (105e). ^{1}H (400 MHz, DMSO-d_6) δ ppm 0.08−0.42 (m, J = 63.5 Hz, 4 H) 0.81−0.91 (m, 1 H) 1.20 (t, 3 H) 1.38 (s, 9 H) 2.65−2.77 (m, 2 H) 3.59 (s, 2 H) 4.09 (q, 2 H) 6.75 (s, 1 H).

Ethyl-5-[(*tert*-butoxycarbonyl)amino]-4-methyl-3-oxopentanoate (105h). Commercially available 3-*tert*-butoxycarbonylamino-2-methyl-propionic acid **98h** (1.34 g, 6.6 mmol), Meldrum's acid (1 g, 6.9 mmol), and 4-dimethylaminopyridine (1.28 g, 10.49 mmol) were dissolved in dichloromethane (70 mL). The reaction mixture was cooled to 0 °C and a solution of 1-(3-dimethylaminopropyl)-3-ethylcarbodiimide hydrochloride (1.47 g, 7.67 mmol) in dichloromethane (50 mL) was added dropwise. The mixture was left at 0 °C overnight. After filtration, the reaction mixture was

washed with 5% aqueous sodium bisulfate (×3) and with brine. The organic extracts were dried over anhydrous sodium sulfate and the solvent was evaporated. The solid (**99h**) was dissolved in ethanol and heated at 70 °C for 6 h with stirring. The solvent was removed and the raw product was purified by flash chromatography (eluant: toluene/ethyl acetate 4:1), affording the title compound as a yellow oil (0.69 g, 38% yield).

^{1}H (400 MHz, DMSO-d_6) δ ppm 0.96 (d, 3 H) 1.16 (t, 3 H) 1.34 (s, 9 H) 2.69−2.84 (m, 1 H) 2.85−3.13 (m, 1 H) 3.15−3.2 (m, 1 H) 4.62 (d, 2 H) 4.05 (q, 2 H), 6.86 (s, 1 H).

Ethyl 2-{2-[(*tert*-Butoxycarbonyl)amino]-3-methylbutyl}-5-pyridin-4-yl-1*H*-pyrrole-3-carboxylate (106b). Ethyl 5-[(*tert*-butoxycarbonyl)amino]-6-methyl-3-oxoheptanoate (7.5 g, 24.9 mmol) and 60% sodium hydride (2.5 g, 62.25 mmol) dissolved in tetrahydrofuran (500 mL) were stirred 1 h at room temperature and then cooled to 0 °C. A suspension of 2-bromo-1-pyridin-4-ylethanone **64a** (8.4 g, 30 mmol) in tetrahydrofuran (120 mL) was added at 0 °C and the mixture was stirred at room temperature for 4 h. After solvent removal, the residue was dissolved in ethanol (300 mL) and ammonium acetate (8.6 g, 124.5 mmol) was added. The solution was stirred or 18 h at room temperature and then was concentrated to dryness. The raw product was dissolved in ethyl acetate, washed (300 mL × 3) with brine and dried over anhydrous sodium sulfate. The solvent was removed and the raw product was purified by flash chromatography (eluant:dichloromethane/methanol 100:2), affording the title compound (3.5 g, 35% yield).

^{1}H (400 MHz, DMSO-d_6) δ ppm 0.92 (d, J = 6.71 Hz, 6 H) 1.19 (s, 9 H) 1.28−1.34 (m, 3 H) 1.67−1.78 (m, 1 H) 2.76−2.87 (m, 1 H) c × 2 H) 8.51 (dd, J = 4.51, 1.46 Hz, 2 H) 11.60 (s, 1 H).

The following compounds were synthesized according to the general procedure detailed above:

Ethyl 2-{2-[(*tert*-Butoxycarbonyl)amino]-2-cyclopropylethyl}-5-pyridin-4-yl-1*H*-pyrrole-3-carboxylate (106e). ^{1}H (400 MHz, DMSO-d_6) δ ppm −0.08−0.37 (m, 4 H) 0.85−0.98 (m, 1 H) 1.23−1.34 (m, 12 H) 2.99−3.38 (m, 3 H) 4.16−4.26 (m, 2 H) 6.56 (d, J = 8.54 Hz, 1 H) 7.10 (d, J = 2.80 Hz, 1 H) 7.64 (dd, J = 4.63, 1.59 Hz, 2 H) 8.50 (d, J = 4.6, 2 H) 11.73 (s, 1 H).

Ethyl 2-{2-[(*tert*-Butoxycarbonyl)amino]-1-methylethyl}-5-pyridin-4-yl-1*H*-pyrrole-3-carboxylate (106h). ^{1}H (400 MHz, DMSO-d_6) δ ppm 1.24 (d, J = 7.19 Hz, 3 H) 1.30 (t, J = 7.07 Hz, 3 H) 1.35 (s, 9 H) 3.78−3.89 (m, 1 H) 4.14 (d, J = 7.13 Hz, 2 H) 6.89 (s, 1 H) 7.09 (d, J = 2.80 Hz, 1 H) 7.71 (d, J = 4.63 Hz, 2 H) 8.51 (d, J = 4.51 Hz, 2 H) 11.48 (s, 1 H).

2. Registry Numbers (RN). 2-Bromo-1-(4-pyridinyl)-ethanone hydrobromide (RN, 5349-17-7), 2-bromo-1-(2-amino-4-pyrimidinyl)-ethanone (RN, 106157-91-9), 3-amino-butanoic acid, (RN, 541-48-0), 3-amino-4-methyl-pentanoic acid, (RN, 5699-54-7), 3-amino-5-methyl-hexanoic acid, (RN, 3653-34-7), β-amino-cyclopropanepropanoic acid (RN, 331633-72-8), 3-amino-4-benzyloxy-butyric acid (RN, 773124-73-5), 3-amino-2-methyl-propionic acid ethyl ester (RN, 22560-81-2), 3-amino-2,2-dimethyl-propanoic acid ethyl ester (RN, 59193-77-0), 3-amino-2-phenyl-propanoic acid ethyl ester (RN, 29754-00-5), DL-aspartic acid β-methyl ester hydrochloride (RN, 1835-52-5), DL-aspartic acid (RN, 617-45-8), ethyl 3-methylcrotonate (RN, 638-10-8), ethyl 2-cyano-2-ethyl butyrate (RN, 1619-56-3), ethyl 2-cyano-3-methyl-2-butenoate (RN, 759-58-0), cyclobutanone (RN, 1191-95-3).

3. Crystallographic Methods. Full-length GSK3β was produced as previously described.[34] Crystals of **89S** in complex with GSK3β grew at 20 °C against a reservoir containing 20% PEG 3350, Hepes pH 8.0, 20 mM $MgCl_2$, and 10% glycerol. **89S** was dissolved in 20% DMSO, 35% PEG 400, 50 mM Hepes pH 7.0, and added at a final concentration of 1 mM to the protein sample. Hanging drops were made by mixing 1 μL of sample with 1 μL of reservoir solution and crystals appeared within one week. Subsequently, larger crystals were obtained via the microseeding method, setting up drops made of 1 μL protein sample, 0.8 μL reservoir solution, and 0.2 μL seed stock. Next, a single crystal was soaked for 20 min in 10 μL of a cryoprotecting solution containing 18% PEG 3350, 25% glycerol, and 20 mM $MgCl_2$ before being flash-cooled in liquid nitrogen.

Diffraction data at 2.2 Å resolution were collected at the ESRF on beamline ID23−1. The crystal belongs to space group $P2_12_12_1$, and two molecules are present in the asymmetric unit (AU). The initial $2mF_o-DF_c$ electron density map prior to the addition of the inhibitor's model clearly showed its binding mode. Moreover, inspection of the electron density after a few cycles of model building/refinement allowed us to unambiguously determine the S configuration of compound **89S**. One point worth mentioning is that, although the electron density is clearly defined, for the majority of the inhibitor, it is somewhat poor for the inhibitor's fluorine atom in both molecules of the AU. Tight NCS restraints were used in Refmac and released at the end of refinement (the atomic coordinates have been deposited in the Protein Data Bank with accession code 3DU8). The final model has an R factor of 21.3% and an R_{free} of 24.6%.

4. Kinase Assays. Kinase assays were performed as previously described.[19]

5. High-Throughput Solubility. Solubility at pH 7 was performed as previously described.[35]

6. Cell Permeability. Caco2 and PAMPA cell permeability assays were performed as previously described.[36]

7. Metabolic Stability. The compound was dissolved in DMSO at 10 mM concentration. Human cDNA expressed cytochrome P450 isoforms (supersomes) were purchased from Gentest (Woburn, MA). Human cytochrome b5 was purchased from PanVera (Madison, WI). All chemicals used were of analytical grade and commercially available. The potential inhibitory effect was investigated against cDNA expressed human CYP1A2, CYP2C8, CYP2C9, CYP2C19, CYP2D6, and CYP3A4 supersomes using typical substrates incubated at their respective K_m concentration. A known inhibitor was included for each CYP isoform to check the inhibition response. These were furafylline, quercetin, sulfaphenazole, tranylcypromine, quinidine, and ketoconazole for CYP1A2, CYP2C8, CYP2C9, CYP2C19, CYP2D6, and CYP3A4, respectively. Analysis of both substrate and metabolite was done by LC/MS-MS.

8. Plasma Protein Binding. Plasma protein binding was performed as previously described.[35]

9. In Vivo Pharmacokinetics. Nu/Nu Mouse. The pharmacokinetic profile of the compounds was investigated in overnight fasted male Nu/Nu mice following a single dose given intravenously (iv) or orally (po). The vehicle used was 5% dextrose solution. A total of six mice were treated (three for each leg). Blood samples of each mouse were collected from the saphenous vein at predose, 0.083, 0.5, 1, 6, and 24 h postdosing following iv dosing, and at predose, 0.25, 0.5, 1, 6, and 24 h following oral dosing. Samples were centrifuged at 10000*g* for 3 min at 4 °C, and the plasma was stored at −80 °C until analysis. Samples were analyzed by LC/MS/MS technique.

Pharmacokinetics for PK/PD Model. CdI Nu/Nu 3 female mice from Charles River Italy, six weeks old, weighing 21−30 g, were treated for 10 days at the dose of 30 mg/kg twice a day. After the last treatment, blood samples were taken at 0.25, 0.5, 1, 3, 6, 24 h postdosing. Samples were centrifuged at 10000*g* for 3 min at 4 °C, and the plasma was stored at −80 °C until analysis. Samples were analyzed by LC/MS/MS technique.

Han-Wistar Rat. The pharmacokinetic profile of the compound was investigated in overnight fasted male Han-Wistar rats, following a single dose given intravenously (iv) or orally (os). The vehicle used was 5% dextrose solution. A total of six rats were treated (three for each leg). Blood samples of each rat were collected from the jugular vein at predose, 0.083, 0.5, 1, 2, 4, 6, and 24 postdosing following iv dosing and at predose 0.25, 0.5, 1, 2, 4, 6, and 24 h following oral dosing. Urine samples were collected in the 0−6 and 6−24 time interval. Plasma samples were centrifuged at 10000*g*

for 3 min at 4 °C, and the plasma was stored at −80 °C until analysis. Plasma and urine samples were analyzed by LC/MS/MS technique.

Beagle Dog. The pharmacokinetic profile of the compound was investigated in overnight fasted male and female Beagle dogs (2/sex). The two treatments (iv and po) were given at the same animals 2-weeks apart. The vehicle used was 5% dextrose solution. Blood samples of each dog were collected from the jugular vein at the following times: predose, 0.083, 0.25, 0.5, 1, 2, 4, 8, 24, and 48 h postdosing following iv dosing and at predose 0.25, 0.5, 1, 2, 4, 8, 24, and 48 h following oral dosing. Urine samples were collected after the following time intervals: 0−8, 8−24, 24−48 h. Plasma samples were centrifuged at 10000*g* for 3 min at 4 °C, and the plasma was stored at −80 °C until analysis. Plasma and urine samples were analyzed by LC/MS/MS technique.

Pharmacokinetic Noncompartmental Data Analysis. The pharmacokinetic parameters were derived by noncompartmental methods using the WinNonlin software program. The highest concentration C_{max} and the time to peak t_{max} were read as the coordinates of the highest observed concentration. The terminal half-life time ($t_{1/2,z}$) was calculated by the formula $t_{1/2,z} = \ln(2)/\lambda_z$, where λ_z is the slope of the terminal linear phase of natural-log concentrations vs time curve. The choice of the points on the terminal phase was based on visual inspection of the data. The area under the plasma level vs time curve, AUC_∞, was calculated by the linear trapezoidal rule up to the last detectable concentration $C(t_z)$ and beyond that time by extrapolation from $C(t_z)$ assuming monoexponential decay, using the following formula: $AUC = AUC(0 - t_z) + C(t_z)/\lambda_z$. The following formulas were applied for the estimate of plasma clearance (CL) and volume of distribution at steady state (V_{ss}). $CL = dose/AUC_\infty$; $MRT = AUMC/AUC_\infty$; $V_{ss} = CL \cdot MRT$; $AUMC = AUMC(0 - t_z) + C(t_z) \cdot t_z/\lambda_z + C(t_z)/\lambda_z^2$, with $AUMC(0 - t_z)$ calculated using the linear trapezoidal rule on $C \cdot t$ vs t plots. The oral bioavailability (expressed as percent) was estimated by the ratio of dose-normalized AUC_∞ values after oral and iv dose. Renal clearance was evaluated as: $A_e/AUCt$, where A_e was the amount of compound excreted unchanged in urine within the scheduled time collection (rat: 0−24 h; dog: 0−48 h).

Pharmacokinetic Compartmental Data Analysis. Pharmacokinetic data for the PK/PD modeling were modeled using a monocompartment with a first-order absorption (k10) and first-order elimination (K01) with the aid of WinNonlin software program.

10. Antiproliferative Assay. HeLa cells (European collection of cell culture) and MCF7 (European collection of cell culture) were cultured in modified Eagle's medium (MEM) supplemented with heat inactivated 10% fetal calf serum (FCS). HCT116 cells (American Type Culture Collection, Manassas, VA) and HT29 (European Collection of Cell Culture) were maintained in McCoy's medium with 10% FCS. SW403 (DSMZ, German Collection of Microorganisms and Cell Cultures) were maintained in DMEM medium with 10% FCS. Normal human dermal fibroblasts (Promocell, Heidelberg, Germany) were maintained in fibroblast basal medium supplemented with growth factors and with 10% FCS. A2780 (European Collection of Cell Culture), COLO205, SW48, NCI-H929 (American Type Culture Collection), and L-363, OPM2 (DSMZ, German Collection of Microorganisms and Cell Cultures), were grown in RPMI1640 10% FCS.

Cells were seeded at different densities ranging from 2500 to 5000 cells/well in 96 well black plates (Perkin-Elmer) with the appropriate complete medium. After 24 h, plates were treated with compounds and incubated for 72 h at 37 °C in 5% CO_2 atmosphere. At the end of incubation, cells were lysed and the ATP content in the well, used as a measure of viable cells, was determined using a thermostable firefly luciferase-based assay (CellTiter-Glo) from Promega. IC_{50} values were calculated using percent of growth versus untreated control.

11. Inhibition of Cell Proliferation. Inhibition of cell proliferation was performed as previously described.[19]

12. Cell Cycle Analysis and BrdU Determination. All the cells in the plates including cells floating in the medium and released during PBS washes were collected and analyzed. Adherent cells were released from the plastic by mild treatment with trypsin and added to the tubes. Cells were washed in PBS and fixed in 70% ethanol in PBS. For FACS analysis, cells were suspended in PBS containing RNase A (2 μg/mL) and propidium iodide (5 μg/mL) and incubated for 30 min at 37 °C. For BrdU staining cells were incubated with 50 μM BrdU, washed in PBS, and fixed in 70% ethanol in PBS. DNA was denatured with 2N HCl for 20 min, and cells were then blocked in buffer containing 1% FCS, 0.5% Tween-20 in PBS and finally incubated with FITC anti-BrdU antibody (Becton Dickinson) diluted 1:5 in the blocking buffer. Samples were analyzed with a FACScan (Becton Dickinson).

13. Western Blot Analysis. For Western blot analysis, cell extracts were prepared in a buffer containing 50 mmol/L Tris-HCl (pH 6.8), 1% SDS, and 1 mmol/L DTT and were sonicated for 10 s. Then 15 μg of protein extract determined by TCA assay was loaded in each lane; anti-MCM2 was from Abcam; anti-caspase3 and anti Rb (pS807/811) were from Cell Signaling; anti-Cdc6 was from Neomarker; anti-pSer53 MCM2 and anti-pSer40/41 MCM2 were previously described.[13]

14. Evaluation of Antitumor Efficacy. CdI Nu/Nu female mice from Charles River Italy, six weeks old, weighing 21−30 g, were maintained in cages with paper filter covers, food, sterilized bedding, and acidified water. A2780 human ovarian carcinoma (from American Type Culture Collection) was maintained by subcutaneous (sc) transplantation in athymic mice using 20−30 mg of tumor brei. For the experiment, tumors were excised and fragments were implanted sc into the left flank. The treatments started when the tumors were measurable; mean tumor weight for all the groups was 0.185 g and **89S** was dissolved in glucose solution. Treatments were administered orally twice a day for 10 days. In the control group, animals were treated with the vehicle twice a day. The tumor growth was evaluated every 3 days. Tumor dimension was regularly measured by calipers during the experiments, and the tumor mass, as well as the PK/PD model parameters, were calculated as described.[37]

The tumor growth inhibition (TGI, %) was calculated according to the equation: %TGI = 100 − (mean tumor weight of treated group/mean tumor weight of control group) × 100. Toxicity was evaluated on the basis of the body weight reduction. Mice were sacrificed when the tumors reached a volume that hampered them, and the gross autopsy findings were reported. 7,12-Dimethylbenz(*a*)anthracene (DMBA) and its vehicle sesame oil were purchased from Sigma-Aldrich. Female CD OFA rats, from Charles River Italy, were intubated with a single intragastric dose of 20 mg of DMBA in 1.0 mL of sesame oil. After approximately 50 days, animals were examined by palpation. When at least one mammary tumor measuring 1 cm in diameter was identified, the rats were placed sequentially into two groups and treated orally, twice a day, for 10 days with 20 mg/kg of **89S**, dissolved in glucose solution or its vehicle. Each group included 10 animals and the volume of Y (control group) or Z (treated group) primary tumors was measured using Vernier calipers for the duration of the experiment.

Acknowledgment. We are grateful to the group of Biochemical Screening, to Dario Ballinari and the colleagues of Cellular Screening and to Nilla Avanzi with the group of Assay Development of Nerviano Medical Sciences. We thank Daniela Borghi, Nicoletta Colombo, Maristella Colombo, Vittorio Pinciroli, and Federico Riccardi Sirtori for NMR and mass determinations, Franco Ciprandi for HPLC purifications, Daniel Brown, Jurgen Moll, Rodrigo Bravo, Nicola Mongelli, Giulio Draetta, and Francesco Colotta for discussion and support.

Supporting Information Available: Elemental analysis results of the target compounds **65**−**97**. This material is available free of charge via the Internet at http://pubs.acs.org.

References

(1) Bell, S. P.; Dutta, A. DNA replication in eukaryotic cells. *Annu. Rev. Biochem.* **2002**, *71*, 333–374.

(2) Diffley, J. F. X. Regulation of Early Events in Chromosome Replication. *Curr. Biol.* **2004**, *14* (18), R778–R786.
(3) Takeda, D. Y.; Dutta, A. DNA replication and progression through S phase. *Oncogene* **2005**, *24*, 2827–2843.
(4) Sato, N.; Arai, K.; Masai, H. Human and Xenopus cDNAs encoding budding yeast Cdc7-related kinases: in vitro phosphorylation of MCM subunits by a putative human homologue of Cdc7. *EMBO J.* **1997**, *16* (14), 4340–4351.
(5) Jiang, W.; Hunter, T. Identification and Characterization of a human protein kinase related to budding yeast Cdc7p. *Proc. Nat. Acad. Sci. U.S.A.* **1997**, *94* (26), 14320–14325.
(6) Hess, G. F.; Drong, R. F.; Weiland, K. L.; Slightom, J. L.; Sclafani, R. A.; Hollingsworth, R. E. A human homolog of the yeast CDC7 gene is overexpressed in some tumors and transformed cell lines. *Gene* **1998**, *211* (1), 133–140.
(7) Jiang, W.; McDonald, D.; Hope, T. J.; Hunter, T. Mammalian Cdc7−Dbf4 protein kinase complex is essential for initiation of DNA replication. *EMBO J.* **1999**, *18*, 5703–5713.
(8) Kim, J. M.; Nakao, K.; Nakamura, K.; Saito, I.; Katsuki, M.; Arai, K.; Masai, H. Inactivation of Cdc7 kinase in mouse ES cells results in S-phase arrest and p53-dependent cell death. *EMBO J.* **2002**, *21*, 2168–2179.
(9) Kumagai, H.; Sato, N.; Yamada, M.; Mahony, D.; Seghezzi, W.; Lees, E.; Arai, K.; Masai, H. A novel growth- and cell cycle-regulated protein, ASK, activates human Cdc7-related kinase and is essential for G1/S transition in mammalian cells. *Mol. Cell. Biol.* **1999**, *19*, 5083–5095.
(10) Montagnoli, A.; Tenca, P.; Sola, F.; Carpani, D.; Brotherton, D.; Albanese, C.; Santocanale, C. Cdc7 inhibition reveals a p53-dependent replication checkpoint that is defective in cancer cells. *Cancer Res.* **2004**, *64*, 7110–7116.
(11) Montagnoli, A.; Bosotti, R.; Villa, F.; Rialland, M.; Brotherton, D.; Mercurio, C.; Berthelsen, J.; Santocanale, C. Drf1, a novel regulatory subunit for human Cdc7 kinase. *EMBO J.* **2002**, *21* (12), 3171–3181.
(12) Masai, H.; Matsui, E.; You, Z.; Ishimi, Y.; Tamai, K.; Arai, K. Human Cdc7-related kinase complex In vitro phosphorylation of MCM by concerted actions of Cdks and Cdc7 and that of a critical threonine residue of Cdc7 bY Cdks. *J. Biol. Chem.* **2000**, *275* (37), 29042–29052.
(13) Montagnoli, A.; Valsasina, B.; Brotherton, D.; Troiani, S.; Rainoldi, S.; Tenca, P.; Molinari, A.; Santocanale, C. Identification of Mcm2 Phosphorylation Sites by S-phase-regulating Kinases. *J. Biol. Chem.* **2006**, *281*, 10281–10290.
(14) Tenca, P.; Brotherton, D.; Montagnoli, A.; Rainoldi, S.; Albanese, C.; Santocanale, C. Cdc7 is an active kinase in human cancer cells undergoing replication stress. *J. Biol. Chem.* **2007**, *282*, 208–215.
(15) Im, J.; Lee, J. ATR-dependent Activation of p38 MAP Kinase Is Responsible for Apoptotic Cell Death in Cells Depleted of Cdc7. *J. Biol. Chem.* **2008**, *283*, 25171–25177.
(16) Chabner, B. A.; Ryan, D. P.; Paz-Arez, L.; Garcia-Carbonero, R.; Calabresi, P. *The Pharmacological Basis of Therapeutics*; McGraw-Hill: New York, 2001; Chapter *52*, 1389−1460.
(17) Bergman, A. M.; Pinedo, H. M.; Peters, G. J. Determinants of resistance to 2′,2′-difluorodeoxycytidine (gemcitabine). *Drug Resist. Updates* **2002**, *5*, 19–33.
(18) Longley, D. B.; Johnston, P. G. Molecular mechanisms of drug resistance. *J. Pathol.* **2005**, *205*, 275–292.
(19) Vanotti, E.; Amici, R.; Bargiotti, A.; Berthelsen, J.; Bosotti, R.; Ciavolella, A.; Cirla, A.; Cristiani, C.; D'Alessio, R.; Forte, B.; Martina, K.; Menichincheri, M.; Molinari, A.; Montagnoli, A.; Orsini, P.; Pillan, A.; Roletto, F.; Scolaro, A.; Tibolla, M.; Valsasina, B.; Varasi, M.; Volpi, D.; Santocanale, C. Cdc7 Kinase Inhibitors: Pyrrolopyridinones as Antitumor Agents. 1. Synthesis and Structure−Activity Relationships. *J. Med. Chem.* **2008**, *51*, 487–501.
(20) Anderson, D. R.; Meyers, M. J.; Vernier, W. F.; Mahoney, M. W.; Kurumbail, R. G.; Caspers, N.; Poda, G. I.; Schindler, J. F.; Reitz, D. B.; Mourey, R. J. Pyrrolopyridine Inhibitors of Mitogen-Activated Protein Kinase-Activated Protein Kinase 2 (MK-2). *J. Med. Chem.* **2007**, *50*, 2647–2654.
(21) Montagnoli, A.; Valsasina, B.; Croci, V.; Menichincheri, M.; Rainoldi, S.; Marchesi, V.; Tibolla, M.; Tenca, P.; Brotherton, D.; Albanese, C.; Patton, V.; Alzani, R.; Ciavolella, A.; Sola, F.; Molinari, A.; Volpi, D.; Avanzi, N.; Fiorentini, F.; Cattoni, M.; Healy, S.; Ballinari, D.; Pesenti, E.; Isacchi, A.; Moll, J.; Bensimon, A.; Vanotti, E.; Santocanale, C. A. Cdc7 kinase inhibitor restricts initiation of DNA replication and has antitumor activity. *Nat. Chem. Biol.* **2008**, *4* (6), 357–365.
(22) Mansour, T. S.; Evans, C. A. Decarboxylative carbon acylation of malonates with aminoacylimidazolides mediated by Lewis acids. *Synth. Commun.* **1990**, *20*, 773–781.
(23) Li, B.; Franck, R. W. Facile Synthesis of N-protected γ and δ-Amino-β-keto-esters. *Bioorg. Med. Chem. Lett.* **1999**, *9*, 2629–2634.
(24) Orsini, P.; Maccario, P.; Colombo, N. Regioselective γ-Alkylation of *tert*-Butyl 2,4-Dioxopiperidine-1-carboxylate. *Synthesis* **2007**, *20*, 3185–3190.
(25) Vanotti, E.; D'Alessio, R.; Tibolla, M.; Varasi, M.; Montagnoli, A.; Santocanale, C.; Orsini, P.; Pillan, A. Pyrimidylpyrrole derivatives active as kinase inhibitors. Patent WO2005/014572, 2005.
(26) Nenitzescu, C. D.; Glats, A. M.; Gavet, M.; Pogany, I. Syntheses of α -substituted β -oxo esters. *Izv. Akad. Nauk SSSR* **1963**, *332*, 339.
(27) Avdeef, A. The rise of PAMPA. *Expert Opin. Drug Metab. Toxicol.* **2005**, *1*, 325–342.
(28) Kansy, M.; Senner, F.; Gubernator, K. Physicochemical High Throughput Screening: Parallel Artificial Membrane Permeation Assay in the Description of Passive Absorption Processes. *J. Med. Chem.* **1998**, *41*, 1007–1010.
(29) Shapiro, G. I. Cyclin-dependent kinase pathways as targets for cancer treatment. *J. Clin. Oncol.* **2006**, *24*, 1770–1783.
(30) Palancade, B.; Bensaude, O. Investigating RNA polymerase II carboxyl-terminal domain (CTD) phosphorylation. *Eur. J. Biochem.* **2003**, *270*, 3859–3870.
(31) Wang, S.; Fischer, P. M. Cyclin-dependent kinase 9: a key transcriptional regulator and potential drug target in oncology, virology and cardiology. *Trends Pharmacol. Sci.* **2008**, *29* (6), 302–313.
(32) Simeoni, M.; Magni, P.; Cammia, C.; De Nicolao, G.; Croci, V.; Pesenti, E.; Germani, M.; Poggesi, I.; Rocchetti, M. Predictive pharmacokinetic−pharmacodynamic modeling of tumor growth kinetics in xenograft models after administration of anticancer agents. *Cancer Res.* **2004**, *64*, 1094–1101.
(33) Colombo, M.; Sirtori, F. R.; Rizzo, V. A fully automated method for accurate mass determination using high-performance liquid chromatography with a quadrupole/orthogonal acceleration time-of-flight mass spectrometer. *Rapid Commun. Mass Spectrom.* **2004**, *18* (4), 511–517.
(34) Bertrand, J. A.; Thieffine, S.; Vulpetti, A.; Cristiani, C.; Valsasina, B.; Knapp, S.; Kalisz, H. M.; Flocco, M. Structural characterization of the GSK3beta active site using selective and non-selective ATP-mimetic inhibitors. *J. Mol. Biol.* **2003**, *333* (2), 393–407.
(35) Pevarello, P.; Brasca, M. G.; Amici, R.; Orsini, P.; Traquandi, G.; Corti, L.; Piutti, C.; Sansonna, P.; Villa, M.; Pierce, B. S.; Pulici, M.; Giordano, P.; Martina, K.; Fritzen, E. L.; Nugent, R. A.; Casale, E.; Cameron, A.; Ciomei, M.; Roletto, F.; Isacchi, A.; Fogliatto, G. P.; Pesenti, E.; Pastori, W.; Marsiglio, A.; Leach, K. L.; Clare, P. M.; Fiorentini, F.; Varasi, M.; Vulpetti, A.; Warpehoski, M. A. 3-Aminopyrazole inhibitors of CDK2/cyclin A as antitumor agents. 1. Lead finding. *J. Med. Chem.* **2004**, *47*, 3367–3380.
(36) Kerns, E. H.; Di, Li.; Petusky, S.; Farris, M.; Ley, R.; Jupp, P. Combined application of parallel artificial membrane permeability assay and Caco-2 permeability assays in drug discovery. *J. Pharm. Sci.* **2004**, *93* (6), 1440–1453.
(37) Bjornsson, T. D.; Callaghan, J. T.; Einolf, H. J.; Fischer, V.; Gan, L.; Grimm, S.; Kao, J.; King, S. P.; Miwa, G.; Ni, L.; Kumar, G.; McLeod, J.; Obach, S. R.; Roberts, S.; Roe, A.; Shah, A.; Snikeris, F.; Sullivan, J. T.; Tweedie, D.; Vega, J. M.; Walsh, J.; Wrighton, S. A. The conduct of in vitro and in vivo drug−drug interaction studies: A PhRMA perspective. *J. Clin. Pharm.* **2003**, *43*, 443–469.

JM800977Q